Enzymology and structure of catalases

Article *in* Advances in Inorganic Chemistry · January 2000

DOI: 10.1016/S0898-8838(00)51001-0

3 authors, including:

Peter Nicholls
University of Essex
218 PUBLICATIONS **5,065** CITATIONS
SEE PROFILE

Ignacio Fita
University of Barcelona
209 PUBLICATIONS **6,127** CITATIONS
SEE PROFILE

ADVANCES IN INORGANIC CHEMISTRY, VOL. 51

ENZYMOLOGY AND STRUCTURE OF CATALASES

PETER NICHOLLS,* IGNACIO FITA,† and PETER C. LOEWEN‡

*Department of Biological Sciences, Central Campus, University of Essex, Wivenhoe Park, Colchester, CO4 3SQ, United Kingdom;
†CID–CSIC, 08034 Barcelona, Spain; and
‡Department of Microbiology, University of Manitoba, Winnipeg, Manitoba R3T 2N2

0898-8838/01 $35.00

I. Introduction

As a result of their striking ability to evolve molecular oxygen, catalases have been the subject of observation and study for well over 100 years with the first report of a biochemical characterization and naming of the enzyme appearing in 1900 (*1*). This history has been well documented (*2, 3*). The overall reaction for the classical enzyme is very simple on paper, $2H_2O_2 \rightarrow 2H_2O + O_2$, but there are two distinct stages in the reaction pathway. The first stage involves oxidation of the heme iron using hydrogen peroxide as substrate to form compound I, an oxyferryl species with one oxidation equivalent located on the iron and a second oxidation equivalent delocalized in a heme cation radical (reaction (1)). The second stage, or reduction of compound I, employs a second molecule of peroxide as electron donor providing two oxidation equivalents (reaction 2).

$$\text{Enz}\,(\text{Por}\text{–}\text{Fe}^{\text{III}}) + H_2O_2 \rightarrow \text{Cpd I}\,(\text{Por}^{+\cdot}\text{–}\text{Fe}^{\text{IV}}\text{=O}) + H_2O \quad (1)$$

$$\text{Cpd I}\,(\text{Por}^{+\cdot}\text{–}\text{Fe}^{\text{IV}}\text{=O}) + H_2O_2 \rightarrow \text{Enz}\,(\text{Por}\text{–}\text{Fe}^{\text{III}}) + H_2O + O_2 \quad (2)$$

Compound I can also undergo a one electron reduction with or without a proton resulting in the formation of an inactive compound II (Reaction (3) or (3a)).

$$\text{Cpd I}\,(\text{Por}^{+\cdot}\text{–}\text{Fe}^{\text{IV}}\text{=O}) + e^- \rightarrow \text{Cpd II}\,(\text{Por}\text{–}\text{Fe}^{\text{IV}}\text{=O}) \quad (3)$$

$$\text{Cpd I}\,(\text{Por}^{+\cdot}\text{–}\text{Fe}^{\text{IV}}\text{=O}) + e^- + H^+ \rightarrow \text{Cpd II}\,(\text{Por}\text{–}\text{Fe}^{\text{IV}}\text{–}\text{OH}^+) \quad (3a)$$

Heme alone can reportedly elicit a catalatic reaction (the reaction mediated by catalase) but at a much reduced, almost negligible, rate compared to the catalatic proteins containing heme, and this may explain the observation of catalase activity in enzymes not normally associated with catalatic activity (*4, 5*). Other enzymes have evolved that can catalyze a similar reaction in the absence of heme, but this review will limit itself to a consideration of heme containing proteins with catalatic activity.

Catalases can also act as peroxidases (catalyzing a peroxidatic reaction) in which electron donors are oxidized via one–one electron transfers (Reactions (4) and (5)).

$$\text{Cpd I}\,(\text{Por}^{+\cdot}\text{–}\text{Fe}^{\text{IV}}\text{=O}) + \text{AH2} \rightarrow \text{Cpd II}\,(\text{Por}\text{–}\text{Fe}^{\text{IV}}\text{–}\text{OH}) + \text{AH.} \quad (4)$$

$$\text{Cpd II}\,(\text{Por}\text{–}\text{Fe}^{\text{IV}}\text{–}\text{OH}) + \text{AH2} \rightarrow \text{Enz}\,(\text{Por}\text{–}\text{Fe}^{\text{III}}) + \text{AH.} \quad (5)$$

Generally, the peroxidatic reaction of true catalases is weak in comparison to actual peroxidases, but can be an important reaction in the class known as catalase-peroxidases (Section II,B).

II. Categorization

The diversity among catalases, evident in the variety of subunit sizes, the number of quaternary structures, the different heme prosthetic groups, and the variety of sequence groups, enables them to be organized in four main groups: the "classic" monofunctional enzymes (type A), the catalase-peroxidases (type B), the nonheme catalases (type C), and miscellaneous proteins with minor catalatic activities (type D).

A. Type A: Monofunctional Catalases

The largest and most extensively studied group of catalases is composed of what are effectively monofunctional enzymes. The dismutation of hydrogen peroxide is their predominant activity and any peroxidatic activity is minor and restricted to small substrates. The most convenient way of subcategorizing this group is based on subunit size with an accompanying attention to heme content. This gives rise to two subgroups, one containing small subunit enzymes (55 to 69 kDa) with heme *b* associated, and one containing large subunit enzymes (75 to 84 kDa) with heme *d* associated. The monofunctional catalases characterized in greatest detail have all proved to be active as tetramers, although dimeric, heterotrimeric, and hexameric enzymes have been reported, but never conclusively characterized. Indeed, the commonality of tetrameric structures (see below), even between the small and large subunit classes of enzymes, demands the presentation of extensive and convincing evidence to confirm any structure that is purported to be other than tetrameric.

A phylogenetic analysis of 70 monofunctional catalase sequences (*6*), now extended to include 113 sequences, has revealed a subdivision into three distinct groups or *clades,* a distinct grouping of sequences arising from a phylogenetic analysis. Clade I contains the plant enzymes and one branch of bacterial catalases. Clade II contains only large subunit catalases with bacterial and fungal origins. Clade III contains a third group of bacterial enzymes as well as fungal and animal enzymes and one enzyme with an archaebacterial origin. The main groupings are supported at very high confidence levels at the main nodes as shown

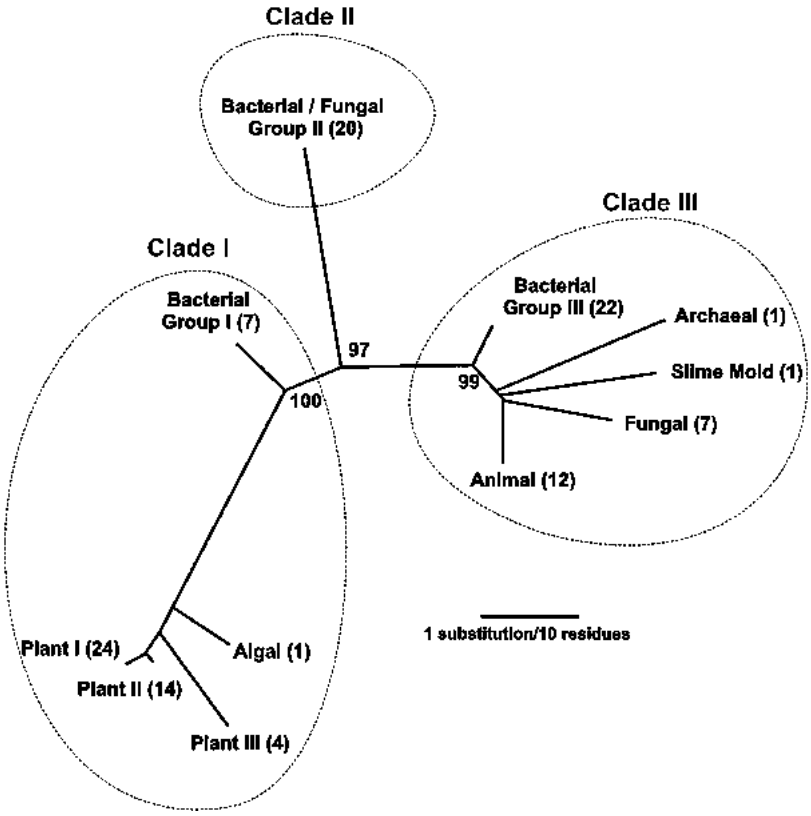

FIG. 1. Unrooted phylogenetic tree based on the core amino acid sequences of 113 catalases. The numbers at the three main nodes represent the proportion (out of 100) of bootstrap sampling that supports the topology. The three main clades are circled for clarity.

in Fig. 1. The inference from such a tree is that the main clades arose from a progenitor catalase through a minimum of at least two gene duplication events. Whether the progenitor enzyme was a large subunit or a small subunit enzyme remains the subject of discussion.

B. TYPE B: CATALASE-PEROXIDASES

The next largest group of catalases are the catalase-peroxidases, so named because they exhibit a significant peroxidatic activity in addition to the catalatic activity. They have been characterized in both fungi and bacteria and resemble certain (type I) plant and fungal peroxidases

in sequence. There is more uniformity in sequence within this group of catalases, which contain heme *b,* have subunits larger than 80 kDa (with a few exceptions), and are active as either dimers or tetramers. It has been hypothesized that the catalase-peroxidases may have arisen through a duplication and fusion event giving rise to two domains with similar sequences in the same subunit (*7*). One of the domains has retained activity and a greater sequence similarity to other catalase-peroxidases, while the second has evolved with greater sequence deviation into an inactive form without bound heme.

A phylogenetic analysis of the catalase-peroxidase sequences (*2*) now extended to 20 available sequences, does not reveal any major subgroupings comparable to those in the catalase family. Whether this is because of the small number of sequences or because of the homogeneity of the enzymes will become evident as further sequences come available. As a result we will, for the time being, refer to the catalase-peroxidases as a single group of enzymes.

C. Type C: Nonheme Catalases

Currently the smallest group, there are only three nonheme catalases so far characterized and an equal number sequenced, all of bacterial origin (*Lactobacillus plantarum, Thermoleophilum album,* and *Thermus thermophilus*). The active site of each of the three enzymes (8–10) contains a manganese-rich reaction center rather than a heme group, and it was this lack of a heme that led to them originally being called "pseudo-catalases." Crystal structures have been determined for the *Lactobacillus plantarum* and *Thermus thermophilus* enzymes (*11*) and have confirmed the active site as containing a bridged binuclear manganese cluster. Its mechanism of catalytic action is currently under discussion. Until more sequences are available, a phylogenetic analysis is not warranted.

D. Type D: Minor Catalases

Several heme-containing proteins, including most peroxidases (*12*), have been observed to exhibit a low level of catalatic activity, with the chloroperoxidase from *Caldariomyces fumago* exhibiting the greatest reactivity as a catalase (*13–15*). Despite the fact that there is as yet only one such example to consider, it provides an alternate mechanism for the catalatic reaction and is addressed in this review. It was first characterized for its ability to chlorinate organic substrates in the presence of chloride and hydrogen peroxide at acid pH, but was later found

to have peroxidatic and catalatic properties above pH 4 in the absence of chloride ion or chloride ion and organic substrate, respectively. The enzyme has a molecular weight of 42 kDa and is active as a monomer. There are three additional classes of haloperoxidases, two of which are nonheme enzymes and are not considered here; the third, including the heme-containing bromoperoxidase from *Streptomyces violaceus,* is considered as a Type A catalase based on its sequence (*16*).

Other proteins such as methemoglobin and metmyoglobin have been observed to produce molecular oxygen in the presence of hydrogen peroxide, but at a very low rate (*5*). This may simply be a property of the heme, which can promote a low-level catalatic reaction in the absence of protein. Consequently, it is possible that all heme-containing proteins may exhibit catalatic reactions if assayed carefully, but such minor, largely nonquantifiable activities are not considered here.

III. Physiology

A. Function

What is the role of catalase in organisms? The obvious is that it protects the organism against reactive oxygen species, particularly those derived from hydrogen peroxide. The existence of so many prokaryotic catalases, as well as their occasional inducibility, suggests that a selective advantage is maintained by the ability to produce and to use catalase intermittently when any organism is liable to experience sudden increases in environmental or internally generated peroxide levels. Cultures of *Escherichia coli* subjected to long periods of aeration die off more rapidly if they lack catalase HPII (hydroperoxidase II) than if it is present (*17*), and Ma and Eaton (*18*) demonstrated a protective role for catalase (HPII or HPI) in *E. coli* cultures. In the latter report, the protection was more evident in dense than in dilute bacterial suspensions, and they speculated that a form of "group protection" against oxidative stress could have been one of the selective forces leading to the evolution of multicellular organisms. Although many populations of *E. coli* may indeed be clonal in character and thus capable of exhibiting group selection characteristics according to conventional Darwinian theory, interpretation of such results in terms of advantage to the individual cell is still possible. The individual cell, even among prokaryotes, is more likely to be at risk from internally generated than externally produced H_2O_2. Internal H_2O_2 may be dissipated either by catalatic activity or by diffusion out of the cell. The amount of catalase expressed in cells

under most conditions will represent the minimum amount required to keep the maximum peroxide concentration during a pulse of production below 0.1 or 0.2 μM (*19, 20*). This can be achieved in *E. coli* by keeping about 0.1% of its total cell protein in the form of catalase. In other microorganisms much higher catalase levels may be needed to preserve a low level of peroxide under all conditions. *Rhodobacter spheroides* can reportedly synthesize up to 25% of its protein in the form of catalase (*21*).

In the case of higher eukaryotes, including humans, Nicholls and Schonbaum (*22*) had suggested that catalase might be a "fossil enzyme," present but without a functional role. This was in part based upon the finding by Aebi *et al.* (*23, 24*) of healthy acatalasics among Swiss Army recruits. One of us (P.N.) remembers the striking photograph of such a soldier, about the same age as himself, and obviously physically far stronger and fitter. Unfortunately, no longitudinal study of these acatalasics seems to have been carried out after Hugo Aebi's death. In the last 35 years we have learned much more about the roles of peroxide-generated free radicals in disease, DNA damage, and aging. P.N. therefore wonders what the Swiss acatalasics of his age look like now.

Enzymes with an intermittent role may be much more important than we thought in 1963. This was perhaps first clearly emphasized by Deisseroth and Dounce in their catalase review of 1970 (*25*). These authors also pointed out the likelihood that the specific location of most eukaryotic catalase in the peroxisomes represents a functional response to the need to decompose hydrogen peroxide generated by the aerobic oxidases present in these same organelles, including hydroxy-acid oxidases and D-amino-acid oxidases.

B. Regulation of Expression

The physiology of catalase expression and its control in bacteria, yeast, and plants has been reviewed elsewhere (*2, 26, 27*). The following precis is presented so that a summary of physiological information relevant to the detailed biochemistry is readily available.

1. Prokaryotes

The early work on catalase expression was carried out largely in *E. coli* and revealed two main response mechanisms. One or the other or both responses have been identified in most other bacteria expressing a catalase. The expected and most obvious response is to oxidative stress. Addition of hydrogen peroxide directly or of ascorbate, which

reacts with oxygen to produce hydrogen peroxide, to the medium of exponential phase cells causes a 10- to 20-fold increase in HPI levels (*28*). This is the result of activation of OxyR, which controls the expression of eight or nine genes encoding enzymes such as HPI and alkylhydroperoxidase (*29*). As cells grow normally through exponential phase into stationary phase, the level of HPI rises about twofold and then falls slightly, a phenomenon that has been attributed, although not without some controversy, to a response to increasing levels of the alternate sigma factor RpoS in stationary phase (*30–32*). Other reagents that impose oxidative stress, such as paraquat, cause a similar response.

A less expected response is the 10- to 20-fold increase in HPII levels as cells grow into stationary phase (*28*). The explanation for this response is that the enzyme serves a protective role during periods of slow or no growth. Indeed, the mutation of *katE* results in strains that die off more rapidly during extended incubation in stationary phase (*17*). The increase in HPII is the result of increasing levels of the alternate sigma factor RpoS, which is a central control element for a generalized stress response, including starvation, acid shock, and hypertonic shift (see review in *33*). The involvement of another transcription factor controlling *katE* expression has never been demonstrated. The levels of RpoS and its influence on transcription are regulated by a complex interplay of factors working at the levels of transcrition, translation, and enzyme stability. Response to oxidative stress and response to other stresses are the two main themes found throughout the prokaryotes, with any variations presumably arising from environmental demands arising from unique habitats.

2. Eukaryotes

Regulation of catalase expression in eukaryotes takes place as part of a generalized response mechanism. In yeast, promoter elements of the peroxisomal catalase CTA-1 respond to glucose repression and activation by fatty acids as part of organelle synthesis. The cytosolic catalase CTT-1 responds as part of a generalized stress response to starvation, heat, high osmolarity, and H_2O_2, and there is even evidence of translational control mediated by heme availability (*26*).

Expression of the multiple catalases in plants (e.g., three in maize and four in mustard) are developmentally controlled, giving rise to complex response patterns. The picture is further complicated by overlapping responses to environmental stresses such as pathogenesis, radiation, hormones, temperature extremes, oxygen extremes, and H_2O_2 (*27*).

IV. Kinetics

A. The Catalatic Pathway

The kinetic behavior of classical catalases remains widely misunderstood, as evidenced by the frequent quoting of K_m and k_{cat}/K_m values for catalases without any rider explaining that these parameters do not have the meaning they possess for standard Michaelis–Menten enzymes, and this continues despite the fact that the matter was effectively clarified more than 50 years ago by Bonnichsen, Chance, and Theorell (*34*). As already described, catalases react with hydrogen peroxide in a two-stage process. In reaction (1), the ferric enzyme combines with hydrogen peroxide to generate water and compound I, the effective enzyme–substrate intermediate or ES, and the rate constant for this reaction is designated k_1. The reverse reaction with a rate constant of k_{-1} is negligible and will not be considered further. In reaction (2), compound I combines with a second molecule of hydrogen peroxide to regenerate the ferric enzyme, molecular oxygen, and water. The rate constant for this reaction is designated k_2, and that for the reverse reaction, which is also negligible and not considered further, k_{-2}. The combined reactions are summarized in Fig. 2A. As both reactions are peroxide-dependent, the simplest model of enzyme activity, that of Bonnichsen, Chance, and Theorell (*34*), predicts that the enzyme is never saturated with its substrate and that the turnover of substrate increases indefinitely as the peroxide concentration increases. This will be referred to as the BCT mechanism.

The velocities of reactions (1) and (2), v_1 and v_2, can be expressed in terms of the total enzyme concentration (or total heme groups) [E] and the concentration of enzyme–substrate complex [ES], as

$$v_1 = k_1[H_2O_2]([E] - [ES]) \tag{6}$$

and

$$v_2 = k_2[H_2O_2][ES]. \tag{7}$$

At steady state these two rates are equal, and we have

$$k_1[H_2O_2]([E] - [ES]) = k_2[H_2O_2][ES], \tag{8}$$

which can be simplified to

$$k_1([E] - [ES]) = k_2[ES]. \tag{9}$$

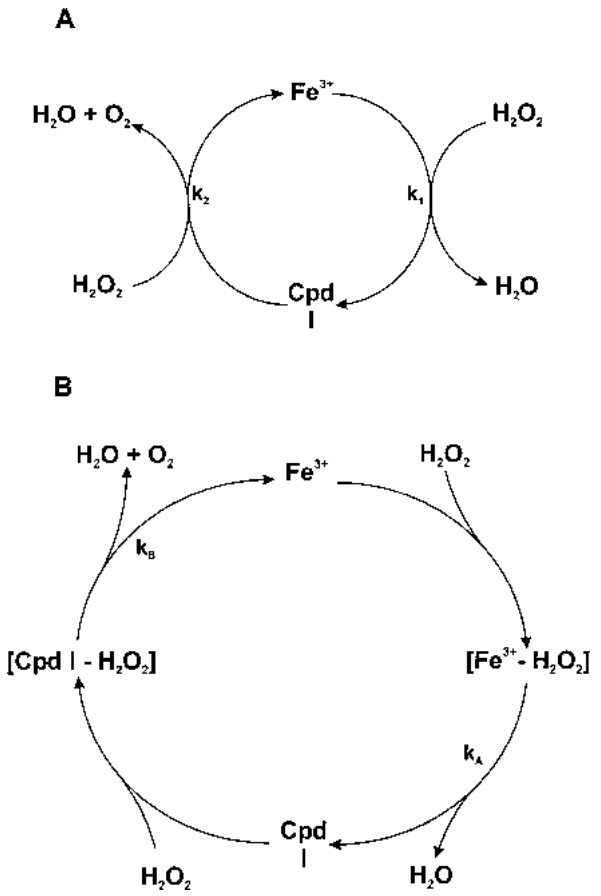

FIG. 2. The Bonnichsen, Chance, and Theorell (*34*) mechanism for the dismutation of hydrogen peroxide by catalase. (**A**) The simple ping-pong mechanism (ferric-peroxide compound cycle) involves only the successive formation and decomposition of the compound I intermediate by two successive molecules of H_2O_2. (**B**) Reversible ES (Fe^{3+}–H_2O_2) and ternary (compound I–H_2O_2]) complexes are added to the mechanism in **A.**

Solving for [ES] gives

$$[\mathrm{ES}] = [\mathrm{E}]k_1/(k_2 + k_1). \tag{10}$$

It follows that the [ES]/[E] ratio is a constant:

$$[\mathrm{ES}]/[\mathrm{E}] = k_1/(k_2 + k_1) = a. \tag{11}$$

Hence, the concentration of the ES complex in the steady state is

independent of $[H_2O_2]$. Reaction 2 or the decomposition of compound I is the rate limiting step resulting in the overall velocity being described by

$$V = 2k_1k_2[H_2O_2][E]/(k_2 + k_1), \tag{12}$$

where the factor 2 is present because each complete cycle involves the loss of two molecules of peroxide. Equation (12) shows that the rate of peroxide decay is proportional to a constant,

$$k' = 2k_1k_2/(k_2 + k_1), \tag{13}$$

multiplied by the product of the concentrations of substrate and enzyme active sites.

Measurement of the overall rate constant, together with a measurement of the steady-state proportion of enzyme that is compound I(a), always permits calculation of the values of the two intrinsic rate constants according to

$$k_2 = k'/2a \tag{14}$$

and

$$k_1 = k'/2(1 - a). \tag{15}$$

The value of k_1 may be determined directly if a trap compound is available that reacts irreversibly and more rapidly with compound I than does a second H_2O_2.

Classical low K_m values for the mammalian enzyme that have appeared in the literature are the result of enzyme inactivation by hydrogen peroxide when measurements were carried out with peroxide levels in excess of 10 mM over time scales of 10 minutes or longer. The rapid sampling/titration method of Bonnichsen overcame the inactivation problem and permitted a satisfactory correlation of the overall catalytic measurements and Chance's observations on the intermediate complex (compound I). Eventually, the introduction of the UV detector/spectrophotometer and the consequent assay based upon the UV absorbance of peroxide (*35*) further simplified the process by eliminating the discontinuous titrimetric assay.

Obviously, there must be a limit to the turnover of any enzyme. Rates cannot theoretically go on increasing indefinitely with substrate concentration. In the case of mammalian catalases, the limits appear to lie in the range between a first order rate of $2 \times 10^6\ sec^{-1}$ and $1 \times 10^7\ sec^{-1}$ (*36*). That is, each heme active site can theoretically decompose between 2 and 10 million molecules of H_2O_2 per second. As two molecules

are decomposed per turnover, that means that the lifetime of the active Michaelis–Menten complex, or compound I, lies between 0.2 and 1 microsecond.

The more complex scheme required if a true K_m is involved is shown in Fig. 2B. There are two possible steps that could provide limiting unimolecular processes, governed by k_A and k_B, the steps involved in formation of compound I and the decay of the "ternary" complex, respectively. Nicholls and Schonbaum (*22*) gave reasons the latter is the preferred limiting step for mammalian catalase. These reasons have not changed much over the past 35 years. But the increased number of catalases examined, especially the catalase-peroxidases, makes reevaluation appropriate (see below).

Several catalases, including the type B catalase-peroxidases, seem to show true substrate saturation at much lower levels of peroxide than originally observed for the mammalian enzyme (in the range of a few millimolar). This means that the limiting maximal turnover is less and the lifetime of the putative Michaelis–Menten intermediate (with the redox equivalent of two molecules of peroxide bound) is much longer. The extended scheme for catalase in Fig. 2B shows that relationships between free enzyme and compound I, and the presumed rate-limiting ternary complex with least stability or fastest decay in eukaryotic enzymes of type A and greatest stability or slowest decay in prokaryotic type B enzymes.

B. The Peroxidatic Activity of Catalases

In addition to their catalatic (peroxide dismuting) activity, catalases also use peroxides to oxidize secondary hydrogen and electron "donor" molecules. There are two major families of possible hydrogen donors: two-electron donors such as alcohols and one-electron donors such as phenols. The two modes of redox behavior are quite distinct. Keilin and Nicholls (*37*) described six donor types, classified according to their reactivities with the two catalase peroxide compounds. Figure 3A shows the basis for this classification. What has happened over the past 40 years to modify this scheme? Firstly, the number of known catalases has increased immensely, but although there are significant quantitative differences in rates of reaction with specific donor types, members of the type A family of catalases, including bovine liver catalase (BLC) and HPII, share many characteristics, including donor specificities. Less complete surveys are available for the more recently discovered catalase-peroxidases or type B enzymes. Secondly, a major development has been the discovery of the special donor role of NADPH

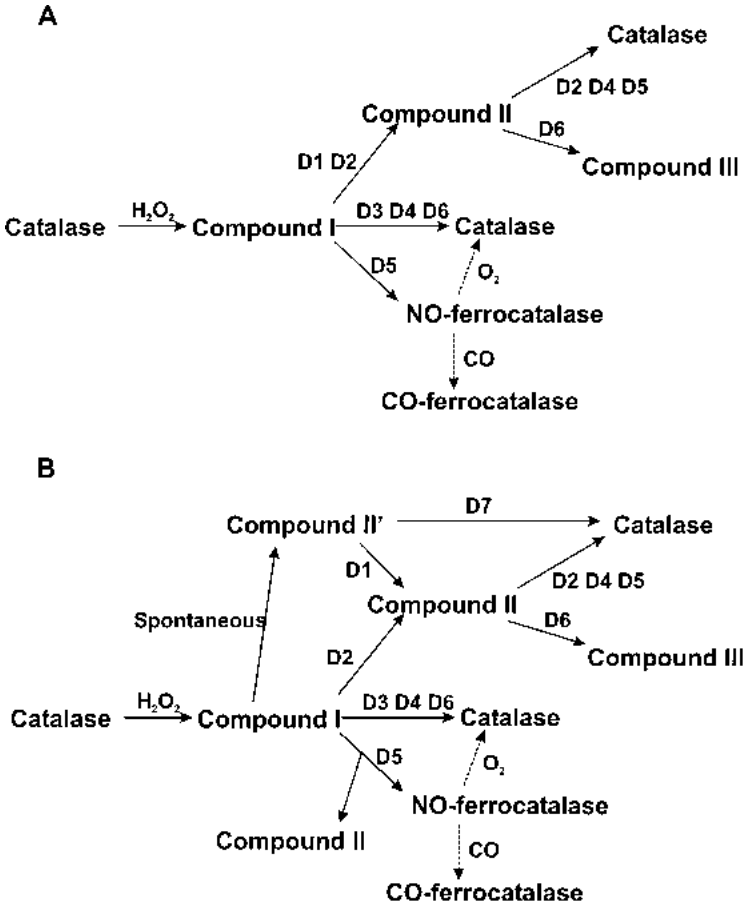

FIG. 3. Classification of catalase hydrogen donors. (**A**) The initial classification proposed by Keilin and Nicholls in 1958 (*37*). D1 donors, including ascorbate and ferrocyanide, reduce only compound I to compound II. D2 donors, including phenols and aromatic amines, reduce compound I to II and compound II to ferric enzyme. D3 donors, including alcohols and formate, reduce only compound I to ferric enzyme. D4 donors, including nitrite, reduce compound I and compound II to ferric enzyme. D5 donors, including azide and hydroxylamine, reduce compound I to ferrous enzyme and compound II to ferric enzyme. D6 donors, including H_2O_2, reduce compound I to ferric enzyme and compound II to compound III. (**B**) A revision of the scheme in part **A** that reflects the inclusion of the new donor group D7, including NADPH and NADH, which reduces a compound II precursor (compound II') to ferric enzyme. In addition, the D1-categorized ferrocyanide is now regarded as primarily a reducer of the compound II' intermediate, and the D5-categorized azide may reduce Fe via an intermediate compound II.

(listed as a seventh donor type below). Thirdly, it has been found that some type A enzymes, including both protoheme forms, such as the enzyme from *Aspergillus*, and chlorin heme forms, such as *E. coli* HPII, appear not to form compound II at all. A fourth modification of the classical scheme involves the observation that certain types of peroxide, such as *t*-butyl hydroperoxide and peroxynitrous acid, may form compound II directly by a homolytic rather than heterolytic split of the O—O bond, with consequent release of a peroxidelike radical into the medium (*t*-butylO$^{\cdot}$ or $NO_2^{\cdot}$). In addition to these overall changes, there have been more detailed changes to the 1958 pathways, as described later.

C. Compound I and the Pathways via Compound I

The visible spectra of beef liver catalase (Type A) and its two active peroxide compounds are shown in Fig. 4. The unliganded enzyme has a Soret band at 405 nm (E_{mM}/heme $\approx$ 120) and a characteristic visible

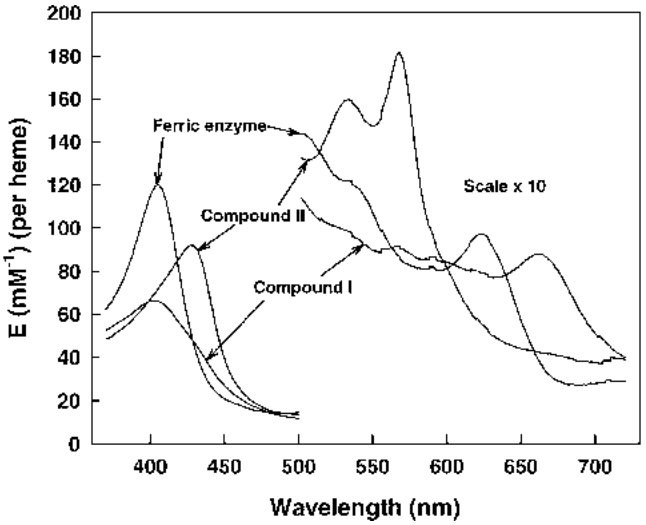

Fig. 4. Visible spectra of catalase, compound I, and compound II; 5 μM (heme) beef liver catalase (Boehringer-Mannheim) in 0.1 M potassium phosphate buffer pH 7.4, 30°C. Compound I was formed by addition of a slight excess of peroxoacetic acid. Compound II was formed from peroxoacetic acid compound I by addition of a small excess of potassium ferrocyanide. Absorbance values are converted to extinction coefficients using 120 mM^{-1} for the coefficient at 405 nm for the ferric enzyme (confirmed by alkaline pyridine hemochromogen formation). Spectra are corrected to 100% from occupancies of $\approx$90% compound I, 10% ferric enzyme (steady state compound I) and 88% compound II, 12% compound I (steady state compound II). The extinction coefficients for the 500 to 720 nm range have been multiplied by 10. Unpublished experiments (P.N., 1999).

spectrum with peaks at 500 and 622 nm and a shoulder at 540 nm, typical of ferric protoheme proteins, differing from the paradigmatic metmyoglobin spectrum by having a long wavelength charge transfer (CT) band at a shorter wavelength and with a higher extinction coefficient, presumably due to the proximal tyrosinate. Compound I, the porphyrin radical-ferryl state (Eq. (1)), is characterized by a much lower Soret peak (E_{mM}/heme $\approx$ 65–70) and a long wavelength band at 665–670 nm, of an intensity almost equal to that of the original CT band, indicating a disruption of the resonating π-bond system of the porphyrin ring. Beyond 700 nm there are absorbances (not shown) due to the presence of heme groups degraded to bile pigments, largely biliverdin with some retention of the heme iron to form verdohemes. Commercial beef liver catalases typically contain up to 45% bile pigment. The structure of the catalase heme groups was originally described as substantially distorted compared to those of other hemoproteins, because these verdoheme structures were averaged with the protoheme ones (*38*).

The donor types D3, D4, and D6 of Keilin and Nicholls (*37*) all reduce compound I of Type A enzymes directly to the ferric state in a two-electron process without detectable intermediates. Each of these donors is probably also able to bind in the heme pocket of the free enzyme. Alcohols (type D3) form complexes with free ferric Type A enzymes whose apparent affinities parallel the effectiveness of the same alcohols as compound I donors (*39*). Formate (type D3) reacts with mammalian ferric enzyme at a rate identical to the rate with which it reduces compound I to free enzyme (*22*). Its oxidation by compound I may thus share an initial step analogous to its complex formation with ferric enzyme. Formate also catalyzes the reduction of compound II to ferric enzyme by "endogenous" donors in the enzyme (*40, 41*). Both compound I and compound II may thus share with the free enzyme the ability to ligate formate in the heme pocket. Nitrite, which is oxidized to nitrate by a two-electron reaction with compound I (type D4), also forms a characteristic complex with free enzyme (*42*). In both cases the reaction involves the donor in its protonated (HNO_2) form.

Hydrogen peroxide itself was given a separate donor status (D6) because in addition to acting like the D3 family and reducing compound I to ferric enzyme in a single two-electron step it can also react with catalase compound II to give the "oxy" or protonated oxy species, compound III (*22*) according to

$$\mathrm{Cpd\,II\,(Por{-}Fe^{IV}{=}OH^{+}) + H_2O_2 \rightarrow Cpd\,III\,(Por{-}Fe^{II}{=}O_2H^{+}) + H_2O.} \qquad (14)$$

Compound III, like compound II, is an inactive form of catalase with respect to the normal catalatic cycle, and thus may contribute to the inactivation of the enzyme at high peroxide levels (*42*).

The classical type A enzymes show marked differences in their abilities to oxidize two-electron donors. All the enzymes initially examined, whether eukaryotic or prokaryotic in origin, were members of clade III. These are rather effective as two-electron peroxidases. But the oxidations of ethanol and formate by the paradigmatic clade II enzyme from *E. coli,* HPII, are much slower. There is little information concerning the activity of type A enzymes in clade I.

There are also substantial differences between classical type A enzymes and the type B catalase-peroxidases. The latter enzymes, although they show peroxidase activity toward donors of type D2, are inactive or only weakly active toward D3 donors such as ethanol.

D. Compound II and the Pathways via Compound II

The visible spectrum of beef liver catalase compound II is also shown in Fig. 4. The enzyme in its one-electron oxidized (ferryl) state has a Soret band at 427 nm (E_{mM}/heme $\approx$ 92) and a characteristic visible spectrum with intense peaks at 533 and 567 nm (E_{mM}/heme $\approx$ 18), indicating a low spin state, differing from the corresponding ferrylmetmyoglobin spectrum by having sharper peaks at a shorter wavelength and with higher extinction coefficients, due either to redox delocalization at the proximal tyrosinate or to protonation of the ferryl species (Eq. (3a)).

The donor types D2, D4, and D5 of Keilin and Nicholls (*37*) all reduce compound II to ferric enzyme in a one-electron process without detectable intermediates. Donors of type D2, phenols and amines, also reduce compound I to compound II. Nitrite, the only member of category D4, reduces compound I in a two-electron step as described earlier. Donors of type D1 reduce compound I to compound II, but have no appreciable effect upon compound II itself. Reactivity of the one-electron donors seems independent of heme pocket binding in the free enzyme.

The donor type D5 comprises the two species azide and hydroxylamine. These both react with the enzyme in the presence of peroxide to give rise to ferrous forms of catalase, otherwise normally inaccessible (catalase is the only common hemoprotein that is nonreducible by dithionite). The final inhibited form of catalase in the presence of azide and peroxide is NO-ferrocatalase, but not every azide molecule becomes an $NO^{\cdot}$; only in the presence of CO is there a stoichiometric inhibition of enzyme by peroxide with formation of 1 equiv of CO-ferrocatalase for every peroxide molecule added (*43*). This suggested a three-electron reduction of compound I either to give ferrocatalase, N_2, and $NO^{\cdot}$ (10–20% total) or to give ferrocatalase, $N^{\cdot}$, and N_2O (80–90% total). However, Kalyanaraman *et al.* (*45*) have demonstrated the formation of the azidyl ($N{=}N{=}N^{\cdot}$) radical in the reaction, and Lardinois

and Rouxhet (*46*) proposed a role for compound II formation in catalase inhibition by azide. Nicholls and Chance (unpublished data) had in fact identified a precursor species closely similar to compound II before the appearance of ferroenzyme. The latter cannot be the result of a second reaction of azide with compound II, as the latter reaction gives rise to ferric enzyme. The simplest hypothesis involves the secondary reaction of the azidyl radical with compound II to give the ferroenzyme with either of two possible breakdown modes of the azidyl radical shown in Fig. 5. The alternative pathway in which the azidyl radical itself reacts with oxygen to give NO and N_2O (*45*) is too slow and does not seem to

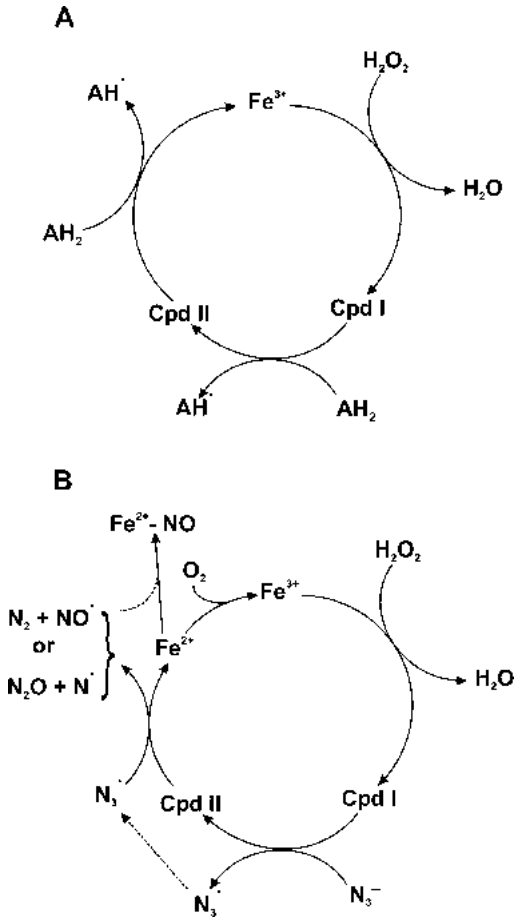

FIG. 5. (**A**) The peroxidatic reaction proceeding via compound II (the D2 family). (**B**) A catalytic cycle involving azide proceeding via compound II and ferroenzyme (the D5 family).

generate a reductant capable of reducing ferric catalase or compound II to the ferro form.

Both classical type A enzymes (clade III) and the heme d family (clade II) show a comparatively high sensitivity to azide inhibition and are reduced to ferrous forms in the presence of peroxide and azide (*47*). In contrast, the catalase-peroxidase (type B) enzymes (see below) are only weakly azide-sensitive.

E. Control by NADPH: The "Extra" Pathway

Kirkman and Gaetani (*48*) discovered the seventh catalase donor type, D7, unknown to Keilin and Nicholls (*37*). In his calculations of *in vivo* or at least "*in erythro*" rates, Nicholls (*49*) had already pondered the possibility of some unusual regeneration pathway for blood catalase, but had vaguely wondered about a role for glutathione, following his original studies on cysteine and glutathione interactions with catalase (*37*). Following the identification of tightly bound $NADP^+$/NADPH by conventional chromatographic methods, Fita and Rossmann (*50*) went back to their data and found that a piece of what previously had been thought to be disordered peptide actually fitted NADPH quite well.

Kirkman and Gaetani (*48*) were able to show not only that tightly bound $NADP^+$ or NADPH was present in mammalian catalases, but also that the presence of the reduced nucleotide decreased compound II formation. The kinetics were, however, anomalous. Of the original families of donors, two types could decrease compound II accumulation: the two-electron D3 category, exemplified by ethanol, which remove compound I before compound II can be formed spontaneously, and the one-electron category (D2), which reduce compound II itself. NADPH falls into neither category. Although it prevents compound II formation from compound I, it does not reduce compound I directly to free enzyme (that is, it is not a conventional two-electron donor), and although it prevents compound II formation, it does not reduce compound II to ferric enzyme once the former species has been produced in its absence. That is, it also cannot act as a one-electron donor. We are presented with an apparent paradox. Hillar and Nicholls (*47*) attempted to resolve the paradox by postulating an intermediate between the compound I and compound II states possessing an unique reactivity with bound NADPH, as indicated in Fig. 6. The initial (slow) step in formation of compound II from compound I lies in the migration of an oxidizing equivalent to a nearby protein residue P (as occurs rapidly and stably, for example, in cytochrome *c* peroxidase). In a second (and relatively rapid) event, the "endogenous" donor centers in the molecule (remote tyrosines, etc.)

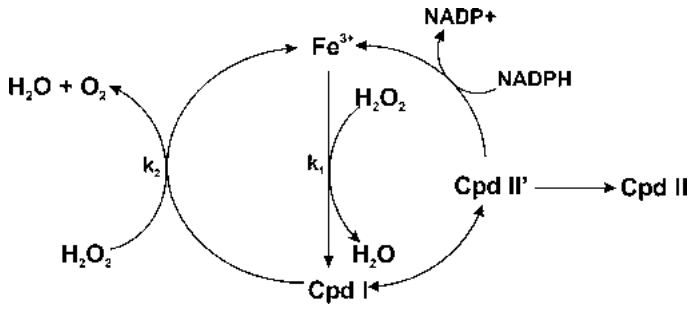

FIG. 6. The catalytic cycle involving a postulated compound II' and NADPH.

reduce the radical P˙ back to its stable PH state. What is PH/P˙? One candidate is the proximal tyrosine, oxidized to the tyrO˙ form with removal of the charged π-electron radical. A second possibility is one of the other nearby tyrosines such as Y235 or Y214 (bovine catalase numbering). A third possibility, suggested by Bicout *et al.* (*51*) (see also Ref. *3*), is that the conserved serine S196 may also act as a radical site. Little seems to be known about serine radicals in any other enzymes, and the likely thermodynamics are therefore hard to estimate.

Two current alternative views are available as to how remotely bound NADPH may work. One sees its action as involving two successive one-electron oxidations (*52, 53*). The effectiveness of NADPH in preventing compound II formation is then due to the high reactivity of the NADP˙ intermediate as reductant of the compound II generated in the first one-electron step. The other model (*47*) prefers to see NADPH as a hydride donor responsible for the almost simultaneous reduction of the ferryl iron and the protein radical species.

Kirkman and Gaetani (*54*) have reexamined the kinetics of NADPH oxidation and compound II formation by mammalian catalase. Under some experimental conditions the rate of NADPH oxidation is substantially higher than the rate of compound II formation in the absence of NADPH. This finding may be accommodated in a scheme such as that of Fig. 6 if the rate of formation of compound II' is greater than the rate of compound II formation. This can arise either if there is more than one route for compound II' decay, only one of which proceeds *via* compound II, or if the formation of compound II' from compound I is reversible, as indicated in the scheme (Fig. 6). Such reversibility is highly probable in view of the redox potentials of the species involved. Although direct measurements have not been carried out with catalases, the corresponding metmyoglobin and horse radish peroxidase peroxide compounds (*55, 56*) have potentials (E'_0 values) of +880 mV (horse radish

peroxidase or HRP comp. I), +900 mV (HRP comp. II), and +890 mV (ferrylmetmyoglobin). Corresponding E_0' values for the trpH/trp$^{\cdot}$ and tyrOH/tyrO$^{\cdot}$ pairs are +1050 and +940 mV, respectively (*57*). Although these potentials may vary in particular proteins, it seems likely that the redox gap between compound I and compound II′ (Fig. 6) will be about 60 mV in favor of compound I. Under the conditions described by Kirkman and Gaetani (*54*), the rate of formation of compound II is approximately 25% the rate of NADPH oxidation. This is consistent with the proposed mechanism provided that the rate of reaction of NADPH (k_5) is fast and the compound I $\rightleftarrows$ compound II′ step is an equilibrium.

The role of NADPH as "protective" donor (*58, 59*) seems to correlate well with the tendency of the different categories of catalases to form the inactive compound II. Only those classical catalases that are vulnerable to the latter inactivation step show $NADP^+$ and NADPH binding. The scheme shown in Fig. 3B summarizes the minimal revisions of the 1958 scheme (Fig. 3A) needed to accommodate the newer findings.

F. The Catalatic Activity of Catalase-Peroxidases

Members of the catalase-peroxidase family were discovered separately in different microorganisms by several groups of workers in the late 1970s and 1980s (*60–62*). It soon became evident that these enzymes are homologous to the eukaryotic type I plant peroxidases of Welinder (*63*). Although these enzymes show both catalase and peroxidase activities and thus obtained the name catalase-peroxidase (CatPx), it is not clear whether their peroxidatic activities are proportionately greater than similar activities shown by classical (type A) enzymes (*64*). What is clear is that the catalatic activity displays several unique distinguishing characteristics. Hochman and Shemesh (*65*) showed that the *Rhodopseudomonas capsulata* enzyme is characterized by instability in presence of the substrate H_2O_2, saturation kinetics ($K_m \approx 4$ mM) for the catalatic reaction, and a relative insensitivity to azide and hydroxylamine.

Follow-up experiments with the similar *Klebsiella pneumoniae* enzyme (*66, 67*) also showed that the pH profiles for CatPx are quite different from those for classical catalases. The latter's catalatic activities are essentially pH-independent from pH 5 to 10 (*68*); CatPx of *Klebsiella* showed a sharp pH optimum between pH 6 and 7 (*66*). A similar eukaryotic fungal CatPx (*69*) was also characterized by a sharp pH sensitivity and saturation kinetics ($K_m \approx 3.4$ mM) and, like the bacterial enzymes, was sensitive to incubation with peroxide but not to the classical catalase inhibitors azide (except weakly) and aminotriazole.

The low peroxidatic activities were less pH sensitive than the catalatic activity.

Most recently, the study of catalase-peroxidases has been extended to the cyanobacteria, which, unlike the eubacteria, seem often to be characterized by possession of only a CatPx (type B) and no type A catalase. Obinger *et al.* (*70*) showed that the *Anacystis nidulans* enzyme had a K_m for H_2O_2 of 4.3 mM and a maximal turnover of over $7000\,sec^{-1}$. At low peroxide levels the activity was about 20% that of beef liver enzyme. Peroxoacetic acid produced a typical compound I species. An analogous enzyme is found in *Synechocystis 6803* (*70, 71*). This enzyme, like the eubacterial examples, shows a narrow pH optimum between pH 6 and pH 7 (*72*) with apparent p*K* values close to 7 and between 5.5 and 6.0. The pH profiles for the peroxidatic activity were different from those for catalatic activity. Again peroxoacetate produces a characteristic compound I. However, the reaction of compound I with one-electron reductants produces a high-spin intermediate different from typical compound II. Regelsberger *et al*. (*71*) also find that the one-electron reduction product obtained by adding ascorbate to compound I is a high spin species with Soret band closely similar to that of free enzyme and visible spectrum with a peak at 626 nm compared to 631 nm for ferric enzyme.

Moreover, the steady-state spectrum in the presence of hydrogen peroxide showed no sign of the presence of compound I (identified from the peroxoacetate spectrum), and compound I produced by peroxoacetate was unaffected by addition of hydrogen peroxide. Regelsberger *et al.* (*71*) and Jakopitsch *et al.* (*72*) nevertheless interpret their results in terms of the classical "BCT" catalatic cycle (Fig. 3), attributing the differences to substantial differences in the kinetic constants for formation and decomposition of compound I, k_1 and k_2 (Eqs. (4) and (5)). An alternative analysis is represented in Fig. 7. Only the peroxidatic activity of the Type B enzymes may proceed via the usual porphyrin–cation radical compound I. The heme configuration, analogous to that of cytochrome *c* peroxidase of yeast, may permit an alternative doubly oxidized state involving a protein radical. If this is the pH-sensitive intermediate, the failure to detect appreciable amounts of compound I during the steady state and the inactivity of peroxoacetate-derived compound I toward H_2O_2 may all be explicable. In addition, the unusual spectrum of compound II of this enzyme may also indicate a more stable protein radical state than the usual ferryl state, even for this intermediate. Electron paramagnetic studies of CatPx enzymes to detect radical states are expected to be undertaken soon that may confirm, refute, or modify this scheme.

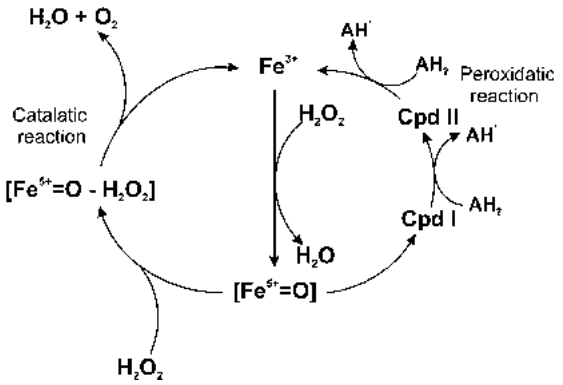

FIG. 7. Catalatic and peroxidatic reactions of type B enzymes. This represents a modification of the schemes of Figs. 2 and 5A and is proposed to account for the characteristic features of catalase-peroxidases. Compound I is drawn as Fe^{5+}═O and can represent either a π-cation radical or alternative radical structure. The precise nature remains undefined (see Section IV,F).

V. Structure of Type A Catalases

Detailed structural information about Type A catalases is available from the crystal structures of seven monofunctional catalases that have been solved. These include representatives from small-subunit clade III enzymes of animal (bovine liver catalase or BLC (*73, 74*) and human erythrocyte (T. P. Ko, submitted to Protein Data Base as file 1qqw)), fungal (*Saccharomyces cerevisiae* SCC-A) (*75, 76*), and bacterial (*Proteus mirabilis* PMC and *Micrococcus lysodeikticus* MLC) (*77, 78*) origins, and large subunit clade II enzymes of fungal (*Penicillium vitale* PVC) (*79, 80*) and bacterial (*E. coli* HPII) (*81, 82*) origins. Despite the differences in size, all six enzymes share a number of common features that appear to be characteristic of catalases, including a homo tetrameric quaternary structure with the heme group deeply buried in a beta-barrel core structure in each subunit.

Within this common core structure, modifications have been identified that provide catalases with further unique properties. The large-subunit enzymes have extensions at both the amino and carboxyl ends, the latter having a flavodoxinlike structure, a unique His–Tyr bond, a protected cysteine, and a modified heme. NADPH binding and an oxidized methionine are found in small subunit enzymes. Identification and assignment of roles to channels providing access to and egress from the deeply buried heme have recently become the focus of study. Analysis of the structure of catalase HPII of *E. coli* has been facilitated by the construction of more than 75 mutants (Table I).

TABLE I

CHARACTERIZATION OF THE HPII MUTANT VARIANTS

Mutation	Specific activity[a] (units/mg)	Heme[b]	His392–Tyr415[c]
Wild type	14,322	*d*	y
Gln3Arg	nd (active)		
Gln3Arg/Glu21Ala	nd (active)		
Gln3Arg/Gly74Ser/Ser75Ala	nd (active)		
Δ(Gln3-Ser20)	np		
Δ(Gln3-Gly34)	np		
Δ(Gln3-Thr50)	np		
Δ(Gln3-Gly74)	np		
(Gln3-Gly74)/Val303Ser/Phe317Ser/ Phe518Ser/Leu571Stop	np		
Glu21Ala	nd (active)		
Gly34Ser/Ser35Ala	nd		
Thr50Ser	nd		
Gly74Ser/Ser75Ala	nd (active)		
His128Ala	<0.1	*b*	n
His128Asn	<0.1	*b*	n
His128Glu	np		
His128Gln	np		
His128Asn/Asn201His	<0.1	*b*	
Ser167Thr	1,100	*d* + *b*	
Ser167Ala	100	*b*	
Ser167Cys	np		
Ser167Asn	np		
Val169Ala	3,788	*d*	y
Val169Ser	3,703	*d*	y
Val169Cys	16	*b*	n
Val169Cys/Cys438Ser/Cys669Ser	10	*b*	
Asp197Ala	14,354	*d*	y
Asp197Ser	14,721	*d*	y
Asp197Ser/His395Gln	15,473	*d*	y
Asn201His	100	*b*	n
Asn201Asp	1,700	*d*	
Asn201Ala	1,300	*d*	
Asn201Gln	50	*d*	
Asn201Arg	np		
Arg260Ala	35,891	*d*	
Arg260Ala/Lys294Ala	12,880	*d*[d]	
Glu270Asp	16,137	*d* + *b*	
Glu270Asp/Glu362His	16,859	*d*	
Ile274Ser	3,416	*d*	
Ile274Ser/Pro356Leu	np		
Ile274Ser/Leu407Met	np		
Ile274Ser/Pro356Leu/Leu407Met	np		
Lys294Ala	18,625	*d* + *b*	

(*continued*)

TABLE I (*Continued*)

Mutation	Specific activity[a] (units/mg)	Heme[b]	His392–Tyr415[c]
Val303Ser	nd		
Phe317Ser	nd		
Pro356Leu	13,220	*d* + *b*	
Pro356Leu/Leu407Met	12,437	*d* + *b*	
Glu362His	18,325	*d* + *b*	
His392Ala	8,875	*b*	n
His392Gln	7,368	*b*	n
His392Glu	4,507	*b* + *d*[d]	n
His392Asp	2,857	*b*	n
His395Ala	9,821	*d*	y
His395Gln	9,224	*d*	y
Leu407Met	12,679	*d* + *b*	
Ser414Ala	5,511	*b* + *d*[d]	y
Tyr415Phe	np		
Tyr415His	np		
Gln419Ala	7,317	*d*[d]	y
Gln419His	11,494	*d*[d]	y
Cys438Ser	7,350	*d*	
Cys438Ala	6,100	*d*	
Cys438Ser/Cys669Ser	8,050	*d*	
Cys438Ala/Cysgg9Ala	12,870	*d*	
Phe518Ser	np		
Leu571Stop	np		
Ile593Stop	np		
Val603Stop	np		
Cys669Ser	10,840	*d* + *b*	
Cys669Ala	7,800	*d*	
Trp742Stop	2,624	*d*	
Arg744Stop	8,600	*d*	
Arg744Ala	8,786	*d*	
Arg744Lys	5,832	*d*	
Arg744Ala/Ile745Stop	6,929	*d*	
Arg744Lys/Ile745Stop	9,284	*d*	
Ile745Stop	13,753	*d*	
Pro746Stop	15,022	*d*	
Lys747Stop	15,349	*d*	
Lys750Stop	15,067	*d*	

[a] nd, not determined; np, insufficient protein accumulated in cells for purification; nd(active), near wild type levels of catalase were noted in crude extracts but enzyme was not purified.

[b] *d,* heme *d; b,* heme *b*. Heme composition was determined by spectral and HPLC analyses. In all cases, the enzymes contained one heme per subunit. Where no indication is given, no determination was made.

[c] Presence of the His392–Tyr415 (y, yes; n, no) covalent bond was determined by MALDI-MS analysis of trypic digest mixtures. Where no indication is given, no determination was made.

[d] There was an increased percentage of the *trans* isomer in these variants.

A. Subunit Structure

The sequences of all catalases exhibit extensive similarity in the core region defined by the β-barrel and active site to the extent that there are 15 invariant residues among 110 catalase sequences, with the variations in an additional 3 probably arising from incorrect sequencing. These include the essential histidine situated in the active site and the essential tyrosine residue that forms the fifth ligand with the heme. Many other residues are highly conserved, varying in only two or three of the catalases. Such extensive similarity speaks to a strong drive for conservation and is suggestive that the three-dimensional structure imposes limitations on the changes that are possible with retention of activity.

The sequence conservation is reflected in a highly conserved secondary and tertiary structure that is most clearly illustrated in the three-dimensional superposition of C^{α} atoms. Ignoring the C-terminal domains of PVC and HPII, the deviation of C^{α} atoms in a superposition of HPII with PVC, BLC, PMC, and MLC results in root mean square deviations of 1.1, 1.5, 1.6, and 1.5 Å for 525, 477, 471, and 465 equivalent centers, respectively (*83*). In other words, there is very little difference in the tertiary structure of the subunits over almost the complete length of the protein. The large and small subunits are shown in Fig. 8 for comparison.

The tertiary structure of small subunit enzymes can be subdivided into four distinct regions, and the C-terminal or flavodoxin domain of the large subunit enzymes becomes a fifth region. These are indicated in Fig. 8 for clarity. The first region is the amino terminal arm (Fig. 8), which extends 50 or more residues from the amino terminus almost to the essential histidine residue (to residue 53 in PMC, 60 in PVC, 73 in BLC, and 127 in HPII). There is very little structural similarity in the N-terminal region and, in the case of HPII, the structure of the terminal 27 residues is not even defined and they do not appear in the crystal structure. Within the N-terminal arm is a 20-residue helix, helix α2 in HPII, which is the first secondary structure element common to all catalases. The presence of helix α1 varies among catalases, and there is no sequence or location equivalence even when it is present.

The second region is the antiparallel β-barrel (Fig. 8) forming the core of the subunit. It includes about 250 residues from the essential histidine toward the C-terminus. The first four strands (β1–4) are contiguous and are separated from the second four strands (β5–6) by three helices (α3–5). The first four strands form the distal side of the heme pocket and portions of the second four strands participate in binding NADPH in small subunit enzymes.

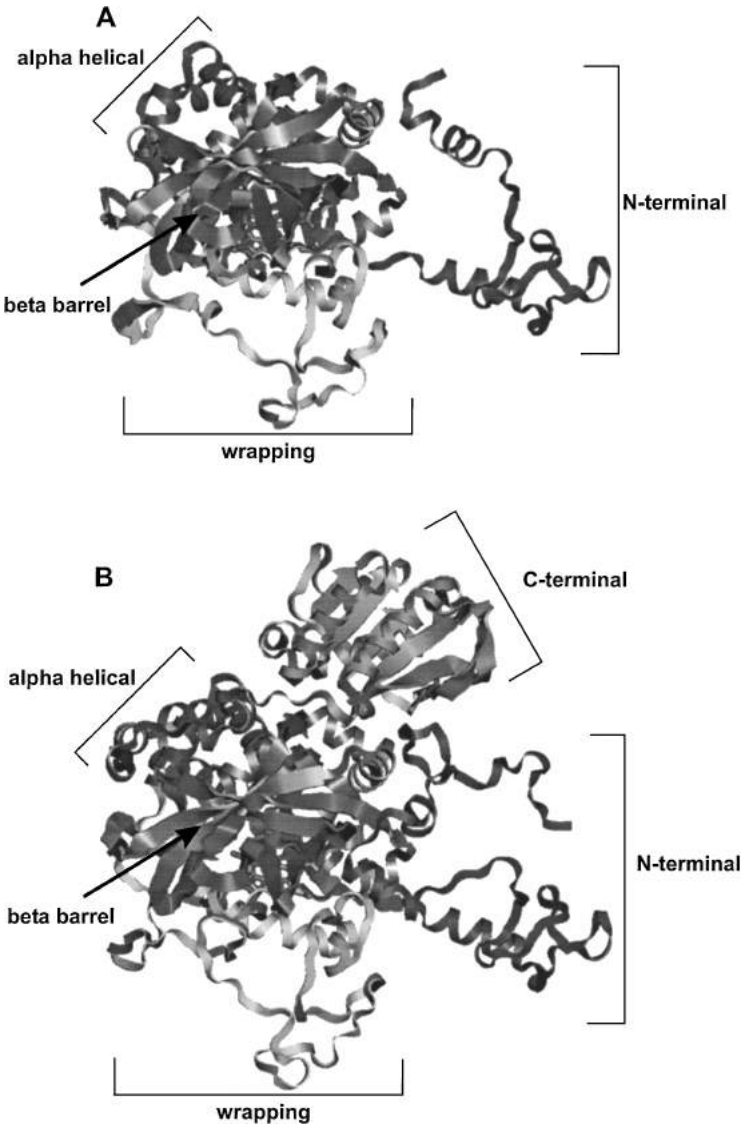

FIG. 8. Comparison of the subunit structures of a small subunit catalase (BLC) (**A**) and a large subunit catalase (HPII) (**B**). Segments including the N-terminal domain, the beta barrel core, the wrapping domain, the alpha helical domain, and the C-terminal domain (HPII) are indicated and are described in Section V,A.

The third region is the wrapping domain (Fig. 8), which includes 110 residues in an extended structure linking the β-barrel and the α-helical section. There is little secondary structure in this region, although helix α9 contains many of the residues that form the proximal side of the heme pocket, including the essential fifth ligand tyrosine. A large surface area for the formation of subunit-subunit interactions is created in this extended structure.

The fourth region is the α-helical domain (Fig. 8) containing about 60 residues organized in four contiguous α helices (α10–13) that form a close association with α-helices 3 to 5 in the β-barrel region to stabilize the structure. This region contains the C-terminus of small-subunit enzymes and, in large-subunit enzymes, may have a critical role in the folding pathway.

In large subunit enzymes (PVC and HPII), a short segment of about 30 residues links the α-helical domain to the C-terminal domain (Fig. 8). The latter segment is a conspicuous addition to the small subunit containing about 150 residues folded into a structure that resembles flavodoxin. For example, there is a root mean square deviation of 3.0 Å between flavodoxin and approximately 100 residues of the C-terminal domains of either HPII or PVC. This can be compared to the 1.8 Å root mean square deviation for 134 centers between the C-terminal domains of HPII and PVC. Unlike the N-terminal end, the final C-terminal residue Ala753 is visible in the structure of HPII. The C-terminal domain contains extensive secondary structure in the form of four α-helices (α15–18) and eight β-strands (β9–16). Despite the obvious structural similarity to flavodoxin, there is no evidence of nucleotide binding in the domain and its function remains a mystery.

Attempts to generate a "small-subunit enzyme" by removing the C-terminal domain of HPII by site-directed mutagenesis were unsuccessful (*84*). Truncation of the subunit at residues 571, 593, or 603 resulted in no protein accumulating in the cell. The lack of protein accumulation was shown to be the result of proteolytic degradation of the protein before it could fold into a protease-resistant form. Even when three hydrophobic residues that would have been exposed by removal of the domain were changed to hydrophilic residues, truncated HPII-like protein did not accumulate. Progressive truncation from the carboxy end revealed that shortening the protein past Arg744 had the same effect as removal of the complete C-terminal domain. The side chain of Arg744 extends into the C-terminal domain and is involved in a number of hydrogen bonds that are clearly important in stabilizing the structure of the domain. These results also show that a properly folded C-terminal domain is essential for the efficient folding of the whole protein into a

stable, protease-resistant structure. Any interference with the folding of the domain interferes with the folding of the whole protein.

B. Quaternary Structure and Interweaving

All seven catalases, which have had their crystal structures solved, exist as homotetramers. Even HPII, which was originally characterized biochemically as a hexamer (*85*), was found to be tetrameric upon solution of the crystal structure. The reason for the biochemical determination of HPII as a hexamer was subsequently traced to the fact that the gel filtration elution volume varies with salt concentration such that elution at low salt results in a larger apparent molecular weight. The consistency in quaternary structure among both large- and small-subunit catalases, that of a tetramer, suggests that variations from the tetrameric structure among heme containing catalases will be rare.

The globular shape of the tetrameric small-subunit enzymes resembles a "dumbbell" in the R–Q orientation (Fig. 9) having dimensions of 90 by 70 by 105 Å along the P, Q, and R axes, respectively, and a "waist" dimension of 50 Å in the $R = 0$ plane. The large subunit enzyme has similar dimensions along the P and Q axes, although with a less obvious "waist," but is 140 Å long along the R axis (Fig. 9). The association of subunits gives rise to an unusual six-stranded antiparallel structure involving all four subunits. Many elements of the quaternary association have been extensively reviewed (*3, 83*).

Perhaps the most unusual feature, and certainly the one that has the greatest implications with regard to the folding pathway and stability of the complex, is the interweaving of adjacent subunits that results in two tightly associated dimers per tetramer. The N-terminal arm of each subunit is folded underneath the wrapping domain of an adjacent subunit and the subunits are oriented such that each "Q-related" dimer pair contains two overlapped interactions (Fig. 10). In the case of small-subunit enzymes such as BLC, about 25 residues of the amino terminus extend beyond the overlap region, and there is very little interaction of those residues with the remainder of the subunit. The length of the overlapped segment is greater in large subunit enzymes such as HPII where 80 residues are "trapped." Furthermore, this longer section forms an extensive network of interactions with the core of the subunit. The more extensive interweaving and N-terminal interactions of HPII predict a more stable structure, and this was corroborated in a study of the denaturation patterns of HPII and BLC (*86*). HPII was activated slightly at temperatures up to 75°C and lost activity in concert with

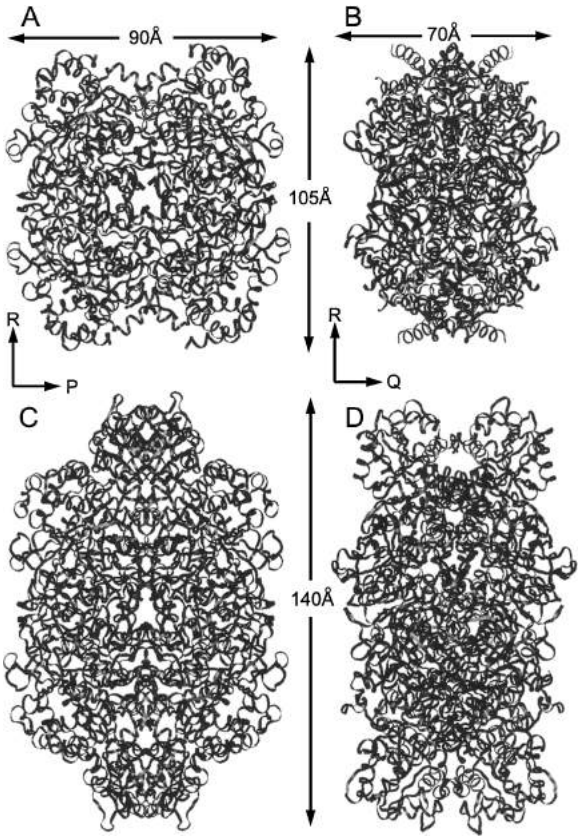

FIG. 9. Comparison of the dimensions of small-subunit (BLC) and large-subunit (HPII) catalases. BLC is shown in panels **A** and **B,** in the *R–P* and *R–Q* orientations, respectively; HPII is shown in **C** and **D,** also in the *R–P* and *R–Q* orientations, respectively.

a transition in secondary structure having a T_m of 82°C. BLC, by comparison, exhibited a similar secondary structure transition and loss of activity, but with a T_m of 56°C (*86*). The most striking illustration of the enhanced stability provided by the interwoven structure is that fact that the dimer structure does not dissociate in potassium phosphate buffer even at 95°C or in 7 M urea, 1% SDS at 60°C (Fig. 11). For comparison, BLC dimers, with the shorter overlapped segment, dissociate at room temperature in the urea–SDS solution.

Bergdoll *et al.* (*87*) have proposed that some proteins, including catalase, exhibit "arm exchange" or an interaction of one subunit with an adjacent subunit to stabilize quaternary structure, and that this

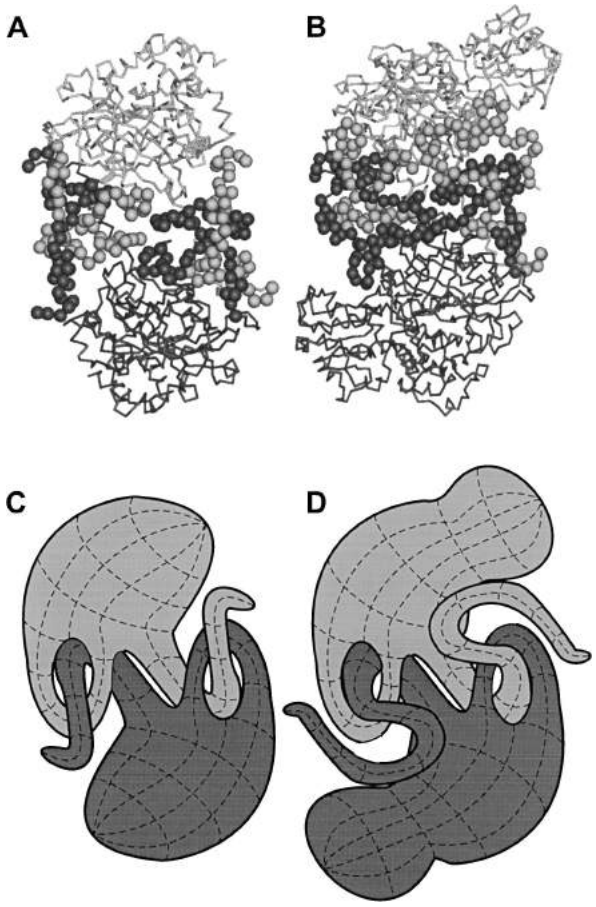

FIG. 10. Illustration of the interweaving of two subunits of the small-subunit BLC (**A**) and the large-subunit HPII (**B**). The residues in the immediate proximity of the overlaps are shown as spheres. A schematic representation of the interwoven structures are shown in **C** for BLC and **D** for HPII. Note the longer N-terminal region of HPII (80 residues in HPII as compared to 25 in BLC) that extend through the loop on the opposite subunit.

interaction is stabilized or enhanced by one or more proline residues. In the case of catalase, Pro69 of BLC, which is highly conserved among all catalases (115 of 117), was identified as the key residue in this interaction. However, the importance of prolines in catalase structure may be far more profound for two reasons. First, the interweaving of subunits in catalases is a more significant interaction than the "arm exchange" interactions or associations identified in other proteins, and, second, far more than one proline are involved when the two proline-

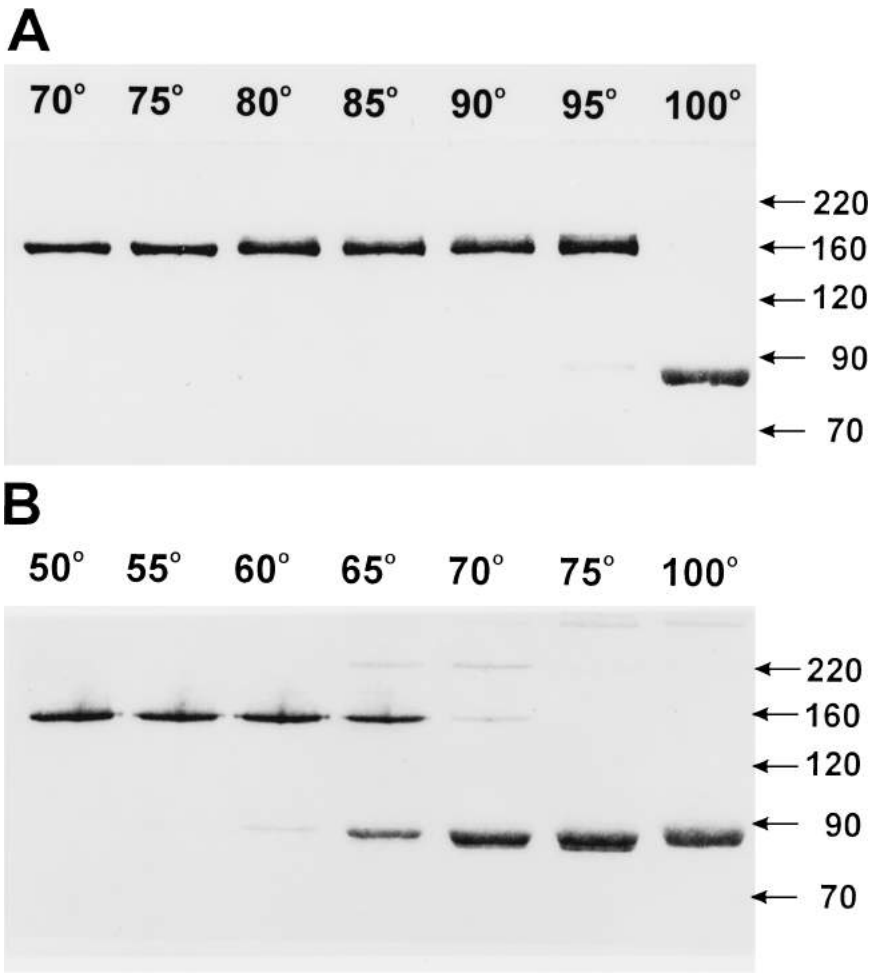

FIG. 11. Conversion of HPII dimers to monomers. In panel **A,** HPII was incubated for 10 min at 70, 75, 80, 85, 90, 95, and 100°C in 50 mM potassium phosphate buffer (pH 7). In panel **B,** HPII was incubated for 10 min at 50, 55, 60, 65, 70, 75, and 100°C in 50 mM potassium phosphate (pH 7) and 5.6 M urea. The temperatures of incubation are indicated above each lane. In both panels **A** and **B,** samples were removed, cooled to room temperature, and added to SDS-urea loading buffer. Samples were loaded and run, without further heating, on an 8% polyacrylamide gel. Reprinted with permission from Switala *et al.* (*86*). Copyright 1999 American Chemical Society.

rich regions surrounding the interwoven regions are considered. This is most evident in HPII, where 10 of 52 residues between 426 and 477, the overlapping segment of the wrapping domain, are proline, and 8 of 28 residues between 31 and 58, in the trapped N-terminal segment, are

proline. There is no equivalent of the N-terminal proline-rich segment in small-subunit enzymes because they lack the N-terminal extension, and this may be another explanation for the enhanced resistance to denaturation of HPII dimers as compared to small-subunit enzymes. These proline-rich segments are in addition to the highly conserved proline identified as Pro69 in BLC (Pro123 in HPII), which may be one more component of this proline network. The prolines would contribute to enhanced rigidity in the overlapped region of the protein and thereby stabilize the quaternary structure. In addition, they may influence the folding pathway as suggested by the folding problems encountered by proteins in which the N-terminal proline-rich region up to residue 50 was deleted (*84*).

The interweaving of subunits necessitates a very complex folding process in which subunit–subunit association must occur before subunit folding is complete. In other words, the formation of secondary, tertiary, and quaternary structural elements are intermixed with quaternary interactions between partially folded subunits being formed before final tertiary and possibly even secondary structural elements can be introduced. A survey of the properties of BLC (*73, 88*), yeast catalase (*89*), and HPII (*84*) provides some insight into the folding process of catalases. For example, dimers formed by BLC have dimensions that would be expected of *R*-related dimers (*88*). Yeast accumulates large quantities of hemeless catalase monomer, and formation of the tetrameric form occurs only after heme is bound by the subunit (*89*). By contrast, HPII requires all portions of its structure to be present for correct folding into an active enzyme (*84*).

A possible mechanism based on these observations is described in Fig. 12. There is an initial folding of domains within the apocatalase, followed by association with the heme, leaving the amino terminal arm, wrapping domain, and alpha helical domain (plus carboxyl domain in large-subunit enzymes) unassociated with the core (A to B in Fig. 12). The requirement for heme early in the folding process may explain why catalases have such a high heme occupancy as compared to the catalase-peroxidases. Following complex formation with the heme, two "*R*-related" subunits will associate (B to C in Fig. 12). The next step involves the association of "*Q*-related" subunits (C to D in Fig. 12). Only one pair of "*Q*-related" subunits is shown in Fig. 12, but there would be two dimers associating simultaneously. During the "*Q*-related" subunit association, the amino terminal arms fold against the subunit, followed by the wrapping such that the α-helical domains (and C-terminal portion) fold overtop of the N-terminal segment to "trap" it (D to E in Fig. 12). In this way, each "*Q*-related" subunit pair will have two interwoven

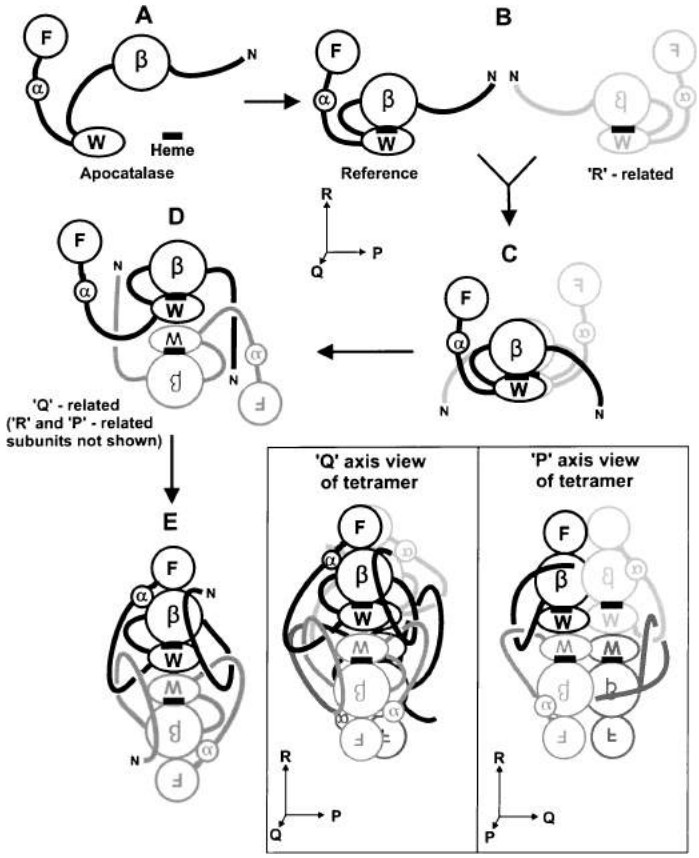

FIG. 12. A hypothetical folding and assembly pathway for catalases. In **A** secondary and tertiary folding first occurs in the individual subunits to form the β-barrel (β), wrapping domain (**W**), α-helical segment (α), and flavodoxin domain (**F,** only in HPII). In proceeding to **B,** heme is bound to each of the subunits, and this may serve as a catalyst for the rapid association of the *R*-related subunits to form the structure in **C.** In proceeding to **D,** *Q*-related subunits associate, resulting in the N-terminal arms being overlapped as the C-terminal portions fold back on themselves to form the fully folded structure shown in **E.** Only two subunits are shown in the progression from **C** to **E,** but a simultaneous folding must be occurring in the associated dimer. The fully folded tetramer is shown in two orientations.

or overlapped segments, and there will be four such interactions per tetramer. The obvious influence of the large-subunit carboxyl terminal domain on the accumulation of protein can be readily explained in such a model, as can be the importance of chaperones (*90*) in stabilizing large segments of unwound or unassociated protein. The initial formation of

the *R*-related dimer shown in Fig. 6 is suggested by the dimensions of the BLC dimer, but the extreme stability of the *Q*-related dimer of HPII suggests that this alternate dimer might form. If this were the case, it would be necessary to change the order in Fig. 12 to B to D to E to tetramer. This is a relatively minor change to the pathway, however, and the main point, that the formation of tertiary and quaternary interactions are intermixed, remains the same. Cartoons of the structures of tetrameric HPII from two different orientations to further illustrate the interactions are also shown in Fig. 12.

C. Heme Composition and Location

The heme of catalases is deeply buried within the core of the catalase subunit. Protoheme IX or heme *b* is found in all small-subunit catalases so far characterized. The two large-subunit enzymes HPII and PVC have been characterized biochemically, spectrally, and structurally (*91*) as containing heme *d* in which ring III is oxidized to a *cis*-hydroxyspirolactone. Heme *b* is initially bound to both enzymes during assembly, and it is subsequently oxidized by the catalase itself during the early rounds of catalysis (*92*).

Another significant difference between the large- and small-subunit enzymes lies in the fact that the heme *d* of HPII and PVC is flipped 180° relative to the heme *b* moiety of BLC, MLC, SCC-A, and PMC (Fig. 13). This is clearly a function of the residues that form the heme pocket, although attempts to force a change in heme orientation in HPII by mutating residues that interact with the heme were unsuccessful. The heme is situated in the β-barrel and has interactions with the wrapping domain and with the amino-terminal arm of the R-related subunit. The dimensions of the pocket demand that heme bind in its final conformation and that flipping once inside the pocket not be possible.

The flipped orientation of the heme in HPII and PVC results in the oxidized ring being sufficiently well removed (7 Å) from the essential histidine (His128 in HPII) and the presumed peroxide binding site to complicate an explanation of the reaction mechanism. The explanation is further complicated by the *cis*-stereospecificity of the reaction that results in both oxygens being situated on the proximal side of the heme away from what is considered to be the normal reaction center on the distal side. This stereochemistry dictates that the hydroxyl group on the heme *d* have originated on the proximal side of the heme, and a mechanism has been proposed to explain the reaction in both PVC and HPII (*93*). The mechanism assumes that compound I is formed as a first step

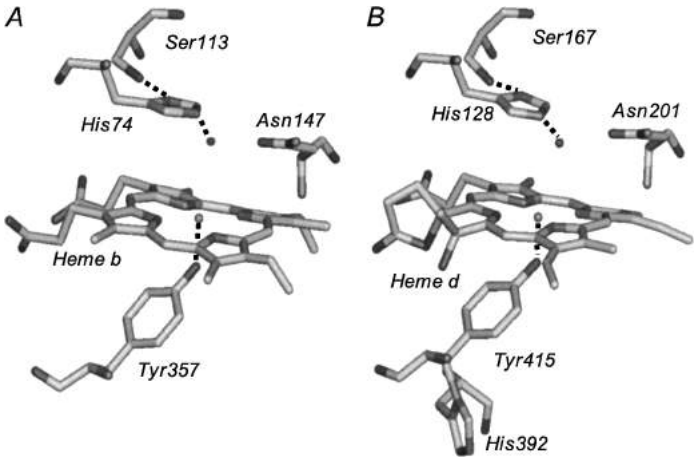

FIG. 13. Active site residues in a small-subunit catalase BLC (**A**) and a large-subunit catalase HPII (**B**). The active site residues are labeled, and hydrogen bonds are shown between the serine (113 in BLC and 167 in HPII) and the essential histidine (74 in BLC and 128 in HPII). A single water is shown hydrogen bonded to the histidine. The equivalent water in BLC is located by analogy to the position of the water in HPII. The unusual covalent bond between the N^{δ} of His392 and the C^{β} of Tyr415 in HPII is evident on the proximal side of the heme in **B.** The flipped orientations of the hemes are evident in a comparison of the two structures, as is the *cis*-hydroxyspirolactone structure of heme d in **B.**

in the heme modification, after which it reacts with a water molecule on the proximal side that acts as an electron donor to the porphyrin cation radical (Fig. 14). Cyclization to form the spirolactone follows completing the reduction of compound I. Water molecules are present on the proximal side, and a potential channel has been identified that would allow access for water. The two residues Ser414 and Gln 419 ensure the *cis* stereochemistry such that changing either residue results in more of the *trans* isomer being formed (*94*).

The mechanism in Fig. 14 applies equally well to both PVC and HPII. However, an unusual bond between the imidazole ring of His392 and the β-carbon of Tyr415 on the proximal side of the HPII heme has been identified (Fig. 13) (*93*), and subsequently its presence was correlated with heme oxidation. The apparent correlation between heme oxidation and His–Tyr bond formation suggested a mechanistic linkage between the two modifications and an alternate mechanism unique to HPII was proposed (Fig. 15). As with the first mechanism, the reaction assumes the formation of compound I that is available for reduction. Formation of the His–Tyr bond, involving a base catalyzed proton extraction from the

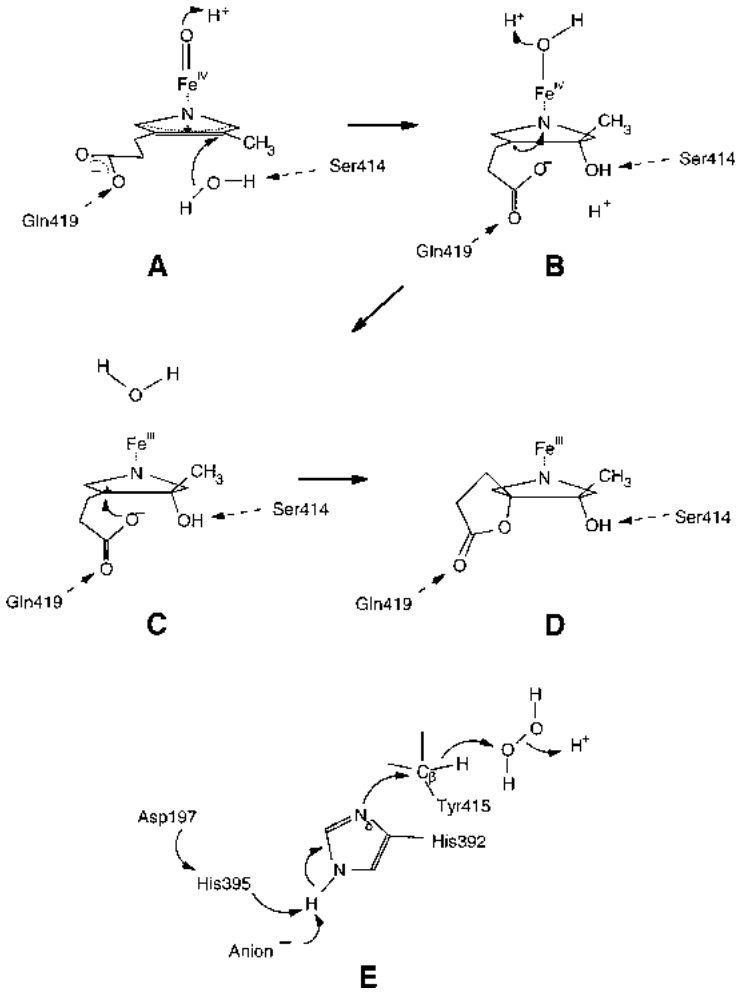

FIG. 14. A mechanism to explain heme modification in the *P. vitale* catalase and possibly *E. coli* HPII. For simplicity, the phenyl ring of Tyr415 is not shown, and only ring III of the heme and the heme iron are shown. Compound I is an oxyferryl species formed, along with water, in the reaction of one H_2O_2 with the heme. The iron is in a formal Fe^V oxidation state, but one oxidation equivalent is delocalized on the heme to create the oxo-Fe^{IV}-heme cation, shown as the starting species, compound I. A water on the proximal side of the heme is added to the heme cation species of compound I shown in **A** to generate a radical ion in **B.** The electron flow toward the oxo-iron would generate the cation shown in (**C**), leading to the spirolactone product shown in **D.** In **E,** an alternate mechanism for the His–Tyr bond formation in HPII is presented that could occur independently of the heme modification reaction. Reprinted with permission of Cambridge University Press from Bravo *et al.* (*93*).

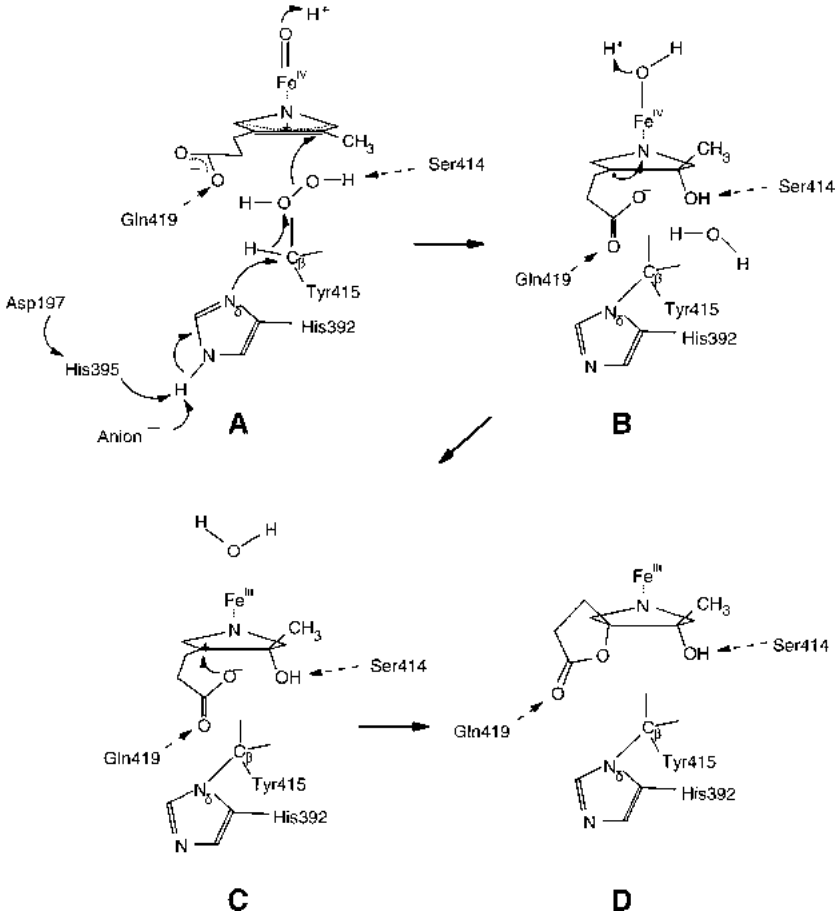

FIG. 15. A proposed mechanism coupling the formation of the His–Tyr bond to the oxidation of ring III of the heme in HPII. The mechanism begins with the formation of compound I shown in **A.** A concerted series of reactions, possibly triggered by either Asp197/His395 or by a putative anionic species bound to compound I, results in the transfer of a hydroxyl to the heme from the H_2O_2 shown in **C,** which would facilitate spirolactone cyclization to form the final product containing the His–Tyr bond and the modified heme shown in **D.** Reprinted with permission of Cambridge University Press from Bravo *et al.* (*93*).

imidazole ring of His392 by a still unidentified species, initiates a concerted reaction that results in peroxide serving as a hydroxide donor to, and consequent reducer of, the porphyrin cation radical (Fig. 15). Subsequent spirolactone formation completes the reduction of the compound I. Supporting the existence of such a mechanism is the observation

that changing His392 to Gln precludes the His–Tyr bond formation and also prevents heme oxidation. Similarly, all inactive variants of HPII in which the heme is not oxidized do not contain the His–Tyr linkage. One exception to this generalization is the His392Glu variant in which some heme oxidation takes place despite the absence of His–Tyr bond formation (*93*). However, even here there appears to be an aberrant reaction pathway because a *trans* hydroxy spirolactone predominates as the oxidized heme. Surprisingly, the *P. vitale* catalase has a Gln in the similar position to the reactive His392 of HPII, but still oxidizes the heme. The conclusion seems to be that despite similar heme structures in HPII and PVC, the mechanisms leading to heme *d* may be different in the two enzymes.

One significant conclusion arising from the characterization of the His392Gln variant of HPII (*93*), which retained near-wild-type levels of activity despite containing heme *b,* is that heme *d* is not required for catalytic activity in the large-subunit enzymes. It is unreasonable to assume that such a modification would have evolved without a reason, but an unambiguous explanation still has not been found. One possibility is that the oxidized form imparts a greater resistance to heme damage and subsequent enzyme inactivation in the presence of high concentrations of hydrogen peroxide. BLC is known to have a significant population of damaged heme (*73*), and it is rapidly inactivated by peroxide concentrations above 300 mM (*95*). By comparison, HPII has nearly 100% occupancy of heme *d* and retains activity in the presence of up to 3 M hydrogen peroxide. The observation that the heme *b*–containing His392Gln variant is no more sensitive to high concentrations of peroxide than the wild-type enzyme would argue against this conclusion, but the possibility of differences in heme damage between the two enzymes after such a treatment has not been determined.

There are a number of relatively invariant residues among the catalases, but four that have been identified over the years as being essential for catalatic activity and integrity of the enzyme are a His (128 in HPII or 74 in BLC),), a Ser (167 in HPII and 113 in BLC), an Asn (201 in HPII or 147 in BLC) and a Tyr (415 in HPII or 357 in BLC), the last forming the fifth ligand with the heme iron. Changing His128 in HPII produced variants that had no detectable activity, confirming that the active site His truly is an "essential" residue for the catalatic reaction. On the other hand, replacements of either Ser167 or Asn 201 resulted in mutant variants with low levels of activity, revealing that the residues facilitated the catalatic reaction but were not "essential." Mutations in Tyr415 abolished the accumulation of any protein, indicating that it was essential for the efficient folding of the protein into a

protease resistant form. Presumably, heme binding is abolished and, in the absence of heme, correct folding of the subunit core does not occur (*92*).

D. Channels and Cavities

The cavity structure of catalases has been extensively analyzed for BLC (*38*), PMC (*77*), PVC (*80*), HPII (*82*), and SCC-A (*76*), revealing a number of large cavities that do not seem to have any role in catalysis. By contrast, smaller pockets exist on the distal side of each of the hemes deeply buried inside each of the subunits that are the active sites of the enzyme. With such deeply buried active site cavities, it is necessary to define access routes that will allow the substrate hydrogen peroxide to penetrate almost 30 Å into the protein. Furthermore, the rapid turnover rate of up to 10^6 per second strongly suggests that there must be separate inlet and outlet channels to allow the rapidly evolving oxygen to be removed without interfering with incoming substrate. The structures of all six catalases reveal two obvious channels leading from the molecular surface to the active site cavity that can fulfill this role. They have been termed major or perpendicular and minor or lateral in the various enzymes. This review will use the terminology "perpendicular" and "lateral" because they clearly describe the orientation of the channels relative to the plane of the heme (Fig. 16). Additional routes for accessing the vicinity of the active site include one leading to the molecular center from the region of the heme propionates and a second leading to the heme proximal side.

The perpendicular channel has long been considered the principal route by which substrate hydrogen peroxide accesses the active site. Two studies of the channel by site-directed mutagenesis have revealed that changes to the largely hydrophobic residues in the lower part of the channel just above the heme do affect enzyme activity in both yeast (*3, 96*) and bacterial catalases (*94*). Enlarging the channel either by changing a valine immediately above the active site histidine to alanine or by replacing phenylalanines with smaller but bulkier aliphatic groups generally causes a decrease in catalatic activity and an increase in peroxidatic activity. These results provide convincing evidence that the channel is used to access the active site. They also reveal that the size of the channel is critical for optimum catalatic activity because enlarging it, which would theoretically increase substrate accessibility, results in a reduction in catalatic activity. On the other hand, the enlarged channel was effective in increasing the peroxidatic activity.

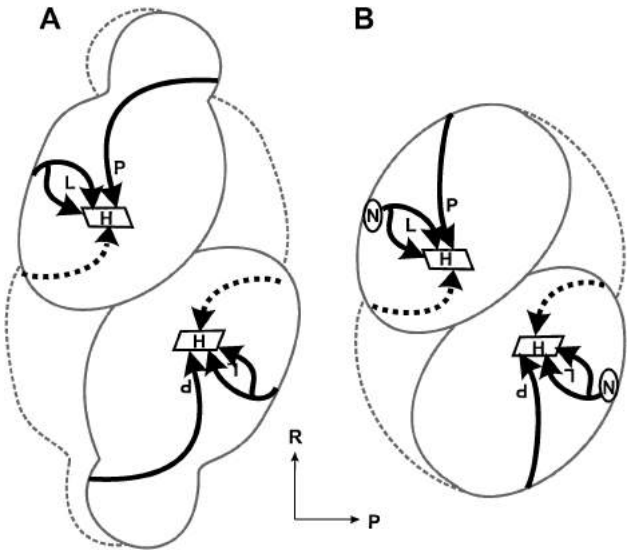

FIG. 16. A cartoon showing the putative channels that provide access to the active site of a large-subunit catalase in **A** and a small-subunit catalase in **B.** The main or perpendicular channel is labeled "**P**" and the minor or lateral channel, which is bifurcated, is labeled "**L.**" A potential channel leading to the proximal side of the heme is shown with a dashed line.

The lateral channel was referred to as the minor channel in part because it was blocked by NADPH in small-subunit enzymes, which created confusion as to whether or not it could act as an efficient channel for substrate or product movement. Furthermore, the channel is really two channels both originating at the site of NADPH binding on the surface of the enzyme. The situation is less complicated in HPII, where NADPH is not bound and the lateral channel provides clear access to the molecular surface. The location in HPII equivalent to the NADPH binding site of small subunit enzymes differs in having Arg260 forming an ionic bond with Glu270, resulting in partial occlusion of the upper branch of the lateral channel. Mutation of Arg260 to Ala significantly enlarges that portion of the channel and results in a threefold increase in specific activity and turnover rate (*95*). Furthermore, alkylated hydroxylamines and sulfhydryl reagents are more effective inhibitors of the Ala260 variant than of the wild-type HPII. It is clear that the inhibitors can access the active site through the lateral channel, but does this mean that the lateral channel also provides access for the substrate hydrogen peroxide to the active site? The answer is not clear.

The enhanced catalatic activity could arise from more facile exhaust of products just as easily as from enhanced substrate accessibility. The effect of inhibitors is a largely static process that is complete once the inhibitor has become bound in the active site. The catalatic process, on the other hand, requires a constant influx of substrate peroxide and efflux of product oxygen and water. As a result, the inlet channels for inhibitors and substrate may be different.

At this time, the proposal of additional access channels is quite conjectural. It seems likely that there is a channel or access route to the proximal side of the heme in order to provide access for the hydrogen peroxide or water needed for heme oxidation and His–Tyr bond formation. Furthermore, the electron density of compound I from PMC (*97*) reveals the presence of an anionic species that is not present in the native enzyme. However, the rapid influx–efflux rates up to 10^6 per sec needed for such a species to be a component of compound I would pose interesting constraints on a channel, and there does not seem to be a likely candidate in the region. Similarly, the potential channel leading to the cavity at the molecular center is not an ideal candidate for substrate or product movement because of its relationship to the active site residues. However, if the lateral channel is truly blocked by NADPH in small-subunit enzymes, this route may provide an alternative access or exhaust route. Both of these latter two channels require further investigation before a clear role can be ascribed to them.

E. NADPH Binding

NADPH seems to be a common component of small-subunit catalases, being present in bacterial (PMC and MLC), yeast (SCC-A and SCC-T), and mammalian (BLC) enzymes. The order of affinity is NADPH > NADH > $NADP^+$ > NAD^+, with one nucleotide bound per monomer. The nucleotide is not a compulsory cofactor and PMC has been isolated and crystallized without the nucleotide bound. This has provided an opportunity to observe that the structural adjustments required for nucleotide binding are minor. The nucleotide binds at a site about 20 Å from the heme iron in an environment that is highly conserved among the small-subunit enzymes. The cavity filled by NADPH in small-subunit enzymes is partially filled in large-subunit enzymes, such as HPII, by a segment (residues 509–595) of the α-helical and linking regions.

The role of the NADPH has not been unequivocally determined. An inactive form of small-subunit enzymes, compound II, can be formed at

low peroxide concentrations as a result of a one-electron reduction of compound I. It has been proposed that NADPH serves as an electron source either to prevent the formation of compound II or to convert the inactive compound II back to the Fe^{III} state, thereby circumventing inactivation (see Section IV,B and IV,E). In the case of large-subunit enzymes, the fact that compound II has never been characterized provides an explanation for why NADPH may not be bound.

NADPH bound to most proteins has an extended conformation that presumably facilitates its role as an electron donor (*98*). However, in catalase NADPH is folded into a much more compact structure, resulting in the adenine and nicotinamide rings being only 3.8 Å apart, although not quite in a stacked conformation. Only the NADPH in flavin reductase P exists in a more compact structure with stacked adenine and nicotinamide rings 3.6 Å apart (*99*). The compact structure in catalase may allow more effective electron donation from the nicotinamide while still allowing the adenine ring to serve as an anchor for the nucleotide on the enzyme surface. The pathway of electron transfer from NADPH to the heme has been the subject of considerable conjecture, including the proposal of protein radical intermediates and of Pro to Ser or Phe to Gly to Ser channeling (*51*). The definitive experiments to characterize the transfer pathway, possibly through the mutation of residues, have yet to be carried out.

The location of NADPH in the lateral channel of small-subunit enzymes blocks the channel such that it cannot realistically be considered to have either an inlet or exhaust function in the presence of the nucleotide. For the channel to have a role in these enzymes, it is necessary to predict that NADPH binds preferentially to the enzyme in its resting state or to inactive forms of the enzyme, such that NADPH is not bound when the enzyme is actively degrading H_2O_2. Thus, the variation in NADPH occupancy among enzymes might reflect the reactive history of the enzyme immediately prior to isolation, as well as the K_a for NADPH binding and the NADPH concentration. For example, enzyme isolated from a culture with high peroxide levels may have a lower amounts of bound NADPH because the enzyme is more active.

F. Complexes

Catalases bind or react with a number of molecules that can be either substrates (hydrogen peroxide and some small alcohols) or inhibitors (cyanide, azide, etc.) (see Section IV,B). Several such intermediates have

been trapped in crystalline form and subjected to structural analysis. Arguably the most interesting is that of the reaction intermediates compound I and compound II of PMC (*97*). Preformed crystals were perfused with peroxoacetic acid, which can oxidize the enzyme to form compound I but cannot reduce it back to the ground state. Subsequent reduction with dithiothreitol converted compound I to compound II.

As would be expected in an enzyme with a turnover rate that can be as high as 10^6 per second, there were no significant rearrangements in the C-alpha backbone structures of compound I and II compared to the ground state enzyme. However, there were two very significant additions of electron density to the structures. One corresponded to the expected ferryl oxygen on the distal side of the heme iron. The second corresponded to the presence of a presumed anionic species replacing a water molecule in a proximal side cavity about 18 Å from the heme iron. The presumption of negative charge was based on the basicity of the cavity and the possibility that it may serve to neutralize the positive charge on the compound I heme. This ion has been implicated as a possible catalyst in the mechanism of His–Tyr bond formation and heme oxidation in HPII (*90*). However, as noted earlier, the concept of ions flowing in and out of the enzyme with each turnover of compound I imposes the requirement of an easily accessible channel. Alternatively, the ion may remain bound while the enzyme is active and dissociate only when activity subsides. One subtle change in the catalytic center involves movement of the heme iron from 0.1 Å below the plane to 0.3 Å above the plane of the heme (*97*).

The only major difference between compounds I and II is the loss of the anion from the proximal side cavity during the formation of compound II. A subtle change in the location of the heme iron from 0.3 Å above the plane to being in the plane of the heme also occurs (*97*). Whether the loss of the putative anion is simply a reflection of the reduced positive charge on the heme in compound II or the explanation for the inactivation of compound II relative to compound I remains undetermined.

The adduct formed between PVC and the inhibitor aminotriazole has been crystallized and the structure determined (G. N. Murshudov, personal communication), providing unequivocal evidence for the mechanism of inhibition. There is a covalent linkage between the essential distal side histidine and the aminotriazole, which remains parallel to the heme forming a hydrogen bond with the active site asparagine. The formation of such a covalent linkage requires that the imidazole ring be oxidized by hydrogen peroxide either directly or indirectly,

possibly involving compound I. No interaction between the heme iron and the aminotriazole is evident. By contrast, the complex of HPII with azide reveals a coordination of the azide molecule between the active site histidine and the heme iron (*83*). No other significant changes in the structure as compared to the wild-type enzyme were noted in either case.

G. Unusual Modifications

Catalases have proven to be a treasure trove of unusual modifications. The first noted modification was the oxidation of Met53 of PMC to a methionine sulfone (*77*). Met53 is situated in the distal side active site adjacent to the essential His54 in a location where oxidation by a molecule of peroxide would not be unexpected. Among the catalases whose structures have been solved, PMC is unique in having the sulfone because valine is the more common replacement in other catalases. The sulfone does not seem to have a role in the catalytic mechanism and is clearly generated as a posttranslational modification. A small number of catalases from other sources, principally bacteria, have Met in the same location as PMC, and it is a reasonable prediction that the same oxidation occurs in those enzymes as well, although this has not been demonstrated.

The subunit of HPII contains two cysteines, 438 and 669, of which Cys438 is situated in the core of the tetramer and Cys669 is situated on the surface of the C-terminal domain. Replacement of the cysteines, either individually or together, causes only small reductions in specific activity of the enzyme, indicating that neither is essential for catalysis or enzyme folding. Analysis of free sulfhydryl groups revealed that Cys448 was blocked and attempts to remove the blocking group were unsuccessful with anything but alkali (*100*). This and other analyses eliminated a number of possible modifications such as acylation, disulfide bonding, oxidation to sulfinic or sulfonic acids, and carbamoylation. Analysis of CNBr digests of HPII and its mutant variants by MALDI mass spectrometry revealed that the peptide containing Cys438 has a mass that is 43 Da larger than expected. As a control, the same peptide from the Cys438Ser variant exhibited the expected mass (allowing for the mutation). An unambiguous identification of the blocking group has not yet been achieved, and the working hypothesis at the moment is that it might involve a hemithioacetal linkage with acetaldehyde. The role of the modification also remains undetermined, although, like the heme oxidation and methionine oxidation in PMC, it may be that the modification increases the enzyme's resistance to inactivation by

hydrogen peroxide. However, the remoteness of the residue from the active site may make this a questionable assertion.

The modification of heme *b* to heme *d* (*91, 92*) observed in the large-subunit enzymes HPII and PVC has already been discussed in detail. Whether all large-subunit enzymes will be found to contain such a modified heme remains to be seen, and the fact that HPII variants containing heme *b* retain activity suggests that naturally occurring large subunit catalases with heme *b* may be found.

The covalent bond linking the N^{δ} of the imidazole ring of His392 to the C^{β} of the essential Tyr415 of HPII (93) has also been described (see Section V,C and Fig. 13). It is found in HPII but not in the closely related large-subunit enzyme, PVC, where the residue equivalent to His392 is a Gln making such a bond impossible. The formation of this unusual bond seems to be linked to heme oxidation, which suggests that its role, like that of heme oxidation, may be to enhance resistance to peroxide, and is therefore another mechanism for stabilizing the enzyme. However, the absence of the covalent bond does not lead to easier denaturation, so it does not contribute measurably to thermal stability. On the other hand, the enzyme has a very rapid turnover rate at high peroxide concentrations, and the added rigidity on the proximal side may help the enzyme to maintain an active conformation in the face of high peroxide concentration or during rapid product formation.

Another unusual covalent bond has been observed in a mutant variant of HPII in which Val169 situated immediately above the essential His128 is changed to a Cys (*94*). The purified variant enzyme exhibits less than 0.1% of wild-type activity, contains heme *b,* and does not contain the His–Tyr bond. The reasons for the lack of activity were clarified only when the crystal structure was solved, revealing a covalent bond between the Cys-S and the C^{δ} of His128. The planar nature of the imidazole ring including the S is suggestive of a retention of sp^2 character or unsaturation in the imidazole ring. The imidazole ring is rotated about 30°, removing it from a being stacked over the heme, thereby interfering with its participation in the catalytic reaction. No other example of such a Cys–His bond has been reported, but the potential exists on the distal side of the heme in the KatE protein from *Xanthomonas campestris,* and this is being investigated.

VI. Structure of Type B Catalase-Peroxidases

The isolation of crystalline catalase-peroxidase has been an elusive goal that so far has not been achieved. The fact that there is no accurate

view of the active sites of the enzyme has complicated a detailed study of the roles of individual residues in catalysis. Fortunately, catalase-peroxidases are similar in sequence to type I plant and fungal peroxidases, particularly in the vicinity of the heme active site. The fact that the structures of a number of peroxidases have been solved has allowed certain assumptions to be made about the identity and location of a number of highly conserved active site residues in the catalase-peroxidases based on analogy with the peroxidase structures.

Heme-containing peroxidases all contain heme *b* with a histidine imidazole as the proximal ligand. On the distal side, a histidine (#52 in cytochrome *c* peroxidase or CCP) and arginine (#48 in CCP) are highly conserved among both peroxidases and catalase-peroxidases. A third position on the distal side of the heme is also highly conserved as either a tryptophan in type I peroxidases (including yeast CCP residue #51) or as phenylalanine in all type II and III peroxidases (including horse radish peroxidase, among others). The orientation of these residues in peroxidases, using CCP as a model, is shown in Fig. 17. The relative positions of the residues in other peroxidases are virtually identical even to the extent that the phenyl and indole rings, respectively, of the phenylalanine and tryptophan options at Trp51 are coplanar when superimposed. The high conservation of these key residues, in three-dimensional orientation among the peroxidases and in sequence among the peroxidases and catalase-peroxidases, provides strong support for the existence of a similar orientation of residues in the catalase-peroxidases including KatG. Furthermore, a recent analysis of the role of these residues in *E. coli* KatG by site-directed mutagenesis of the key Arg, His, and Trp

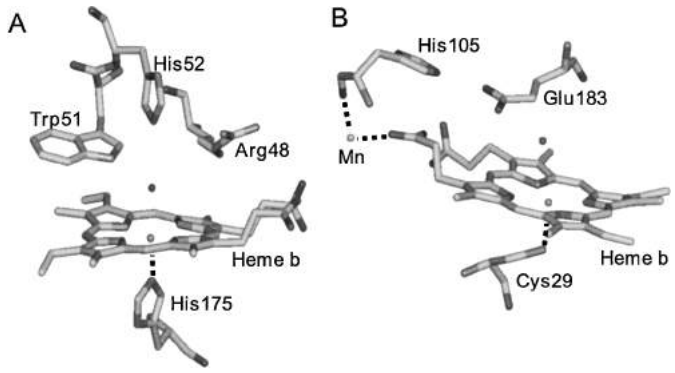

FIG. 17. Active site residues in yeast CCP (**A**) and chloroperoxidase (**B**). The active site residues are labeled, and a single water identified in the electron density situated over the heme iron is shown.

residues has confirmed that they are involved in the catalytic mechanism (*101*). The role of these residues in the catalatic mechanism is discussed later.

VII. Structure of Chloroperoxidase

The crystal structure of the monomeric chloroperoxidase from *C. fumago* has been determined (*14*), revealing a gross structure and active site that are very different from those of other catalases and peroxidases. The enzyme exists as a 42-kDa monomer containing one heme *b* group bound in an eight-helical-segment array. Within the active site and from a mechanistic standpoint, the most significant differences lie in the proximal side fifth ligand to the heme iron, which is a cysteine, rather than histidine or tryptophan, and in the presence of a single catalytic residue on the distal side of the heme, glutamic acid, rather than histidine in combination with asparagine or arginine as in catalases or catalase-peroxidases, respectively. There is a histidine on the distal side of the heme, but it is situated above the propionate side chains of the heme, seemingly too far away from the heme iron to participate directly in the formation or reduction of compound I (Fig. 17). In addition, there is a Mn^{II} associated with the heme propionates and His105, but its role is unknown.

VIII. Mechanism of the Catalatic Reaction

A. Compound I Formation

The first mechanism for the formation of compound I by either a peroxidase or a catalase was proposed in 1980 by Poulos and Kraut (*102*) based on the then newly determined structure of cytochrome *c* peroxidase. This has been reviewed recently (*103, 104*). It remains the operative mechanism for peroxidases with similar active sites and has been adapted to explain the catalatic reaction. In CCP, Arg48 and His52 on the heme distal side were identified as the catalytic determinants that bind and polarize the hydrogen peroxide molecule in concert with the heme iron. The imidazole ring of His52, which is oriented perpendicular to the plane of and about 6 Å above the heme, acts as a proton acceptor from the hydrogen peroxide, while the Arg side chain, which is situated laterally across the heme from the imidazole, stabilizes the charged intermediates. The resulting oxyferryl compound I has the iron oxidized

to Fe^{IV} and has a second oxidation equivalent in the form a protein radical situated on the proximal Trp191, although in some peroxidases such as HRP, the second oxidation equivalent is found as a porphyrin cation radical. As already described, the structure of the active site of type B catalase-peroxidases is based on analogy with the active site of peroxidases. Consequently, any mechanism proposed for compound I formation will, by necessity, be similar to the mechanism proposed for CCP. That is, the His and Arg residues, 106 and 102, respectively, in HPI, participate in a polarization of the O—O bond and proton transfer to produce compound I (Fig. 18A). The electronic structure of compound I in HPI remains unclear, and there is even the potential for two different compound I species depending on the reaction pathway (see Section

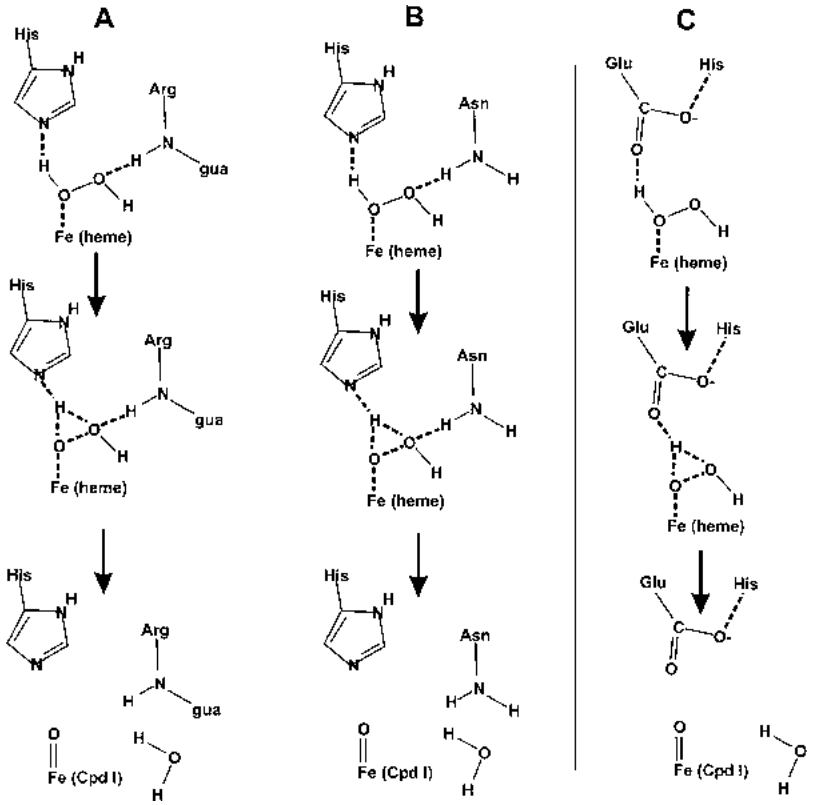

FIG. 18. Mechanisms of compound I formation in type B catalases (based on yeast CCP) (see also Section IV,F and Fig. 7) (**A**): type A catalases (**B**); and chloroperoxidase (**C**).

IV, F and Fig. 7). In catalatic mode, HPI exhibits no significant spectral change, suggesting that compound I has an oxidation equivalent in the form of a protein radical rather than a porphyrin radical. On the other hand, the W105F variant of HPI, which operates only in peroxidatic mode, has a porphyrin radical clearly evident in the absorbance and EPR spectra (*101*).

The mechanism for compound I formation in catalases is very similar to that just described for peroxidases. The active site of a type A catalase also has a histidine, which is essential for catalytic activity, and an asparagine, which, although not essential, greatly enhances catalysis (*92*). Despite the orientations of the active site residues of catalase, particularly the histidine, differing significantly from the orientations of the equivalent residues in peroxidases, the histidines have similar roles in both enzymes while the asparagine of catalase plays a role similar to the arginine of peroxidase (Fig. 18B). In contrast to its orientation in peroxidases, the imidazole of the essential histidine in catalases is coplanar with the heme, effectively stacked, about 3.5 Å above ring III of heme *b* in BLC or ring IV of heme *d* in HPII. Like the arginine in peroxidases, the asparagine residue is situated laterally across the heme from the histidine in a position where it can hydrogen bond with the hydrogen peroxide during catalysis. The presence of similar residues allowed the catalatic mechanism to be modeled on the peroxidatic mechanism (*38*). Interaction of the hydrogen peroxide with both the heme Fe^{III} and the imidazole ring of the histidine weakens and stretches the O—H bond, allowing the second oxygen of the peroxide to simultaneously form a hydrogen bond with the imidazole. The proton on the O that is interacting with the Fe is then transferred, via the imidazole, to the second oxygen, giving rise to water and compound I. The asparagine residue participates through hydrogen bonding with the peroxide and stabilizes the polarized intermediates.

For chloroperoxidase, a type D catalase, the mechanism for compound I formation must differ significantly from those just described because the only active site residue sufficiently close to the heme iron to participate directly in the reaction is glutamate183. The glutamate is hydrogen bonded with His105, but the latter is too distant to participate directly in the reaction with hydrogen peroxide. Therefore, the hydrogen peroxide must initially associate in the active site with the heme Fe^{III} and the glutamate side chain. As the reaction progresses, a second hydrogen bond may form with the highly electronegative glutamate side chain to facilitate proton transfer from the Fe—O—H to the second O, producing water and compound I (Fig. 18C). Even making allowances for possible differences arising from assays in different laboratories, the

catalatic activity of the chloroperoxidase is not more than 2% that of type A or B catalases, suggesting that the active site of the chloroperoxidase is not optimized for the catalatic reaction, consistent with it being a side reaction.

The reaction of other minor or type D catalases such as methemoglobin and metmyoglobin is not treated in detail here, because they are minor activities, significantly lower than even that of chloroperoxidase. The orientation of residues on the distal side of the heme is not optimized for the catalatic reaction to the extent that there is even a sixth ligand of the heme, a histidine, that would preclude a close association of the heme with hydrogen peroxide without a significant side-chain movement. It is only after an extended treatment with H_2O_2 and oxidation of the Fe that a low level of catalatic activity becomes evident.

B. Compound I Reduction

The mechanism for the reduction of compound I by catalases must differ significantly from the mechanism in peroxidases because of the involvement of hydrogen peroxide as the two-electron donor rather than sequential organic substrates acting as one-electron donors. Based again on the peroxidatic reaction, the catalase-peroxidase or type B catalases were initially thought to employ Arg102 and His106 (HPII numbering) as catalytic residues in the reduction stage. However, recent evidence suggests that the active site tryptophan, Trp105 in HPI, plays an important role. Removal of Trp105, while not affecting compound I formation to the extent that compound I could be identified by absorbance and EPR spectrometry, significantly inhibits its subsequent reduction by hydrogen peroxide (*101*). Because it is not possible for hydrogen peroxide to bind simultaneously to all three of His106, Trp105, and Arg102, a modified second stage is proposed in which the indole ring of Trp105 has a role analogous to that of the active site Asn in type A catalases. Along with the imidazole of His106, it binds the second hydrogen peroxide and facilitates hydrogen transfer to the oxyferryl oxygen and to the imidazole ring of His106. The final transfer of the second reducing equivalent, from the imidazole of His106 to the Fe—O—H, completes the cycle, producing water and native enzyme (Fig. 19A). This mechanism is independent of the protein and porphyrin radical structure of compound I (see Section IV,F and Fig. 7).

In the type A catalases, there are only two active site residues in locations where they can influence the reaction, a histidine and an asparagine. A mechanism for compound I reduction in catalases was

propsed by Fita and Rossmann (*38*) in BLC involving these two residues. The hydrogen peroxide binds to compound I, forming hydrogen bonds with the oxyferryl oxygen, the His imidazole, and the Asn side chain. This structure allows the transfer of one hydrogen to the oxyferryl oxygen and a second to the imidazole, resulting in formation of oxygen. The hydrogen and second reducing equivalent on the imidazole ring could then be transferred to the Fe^{IV}–OH to produce water and regenerate the enzyme in its native state (Fig. 19B). The role of the Asn in this stage might be to stabilize the nascent oxygen during the reaction. Direct evidence for this portion of the mechanism is lacking, although the Asn201His variant of HPII exhibits spectral changes consistent with a modification of the heme environment despite a very low catalatic activity and no oxidation of the heme (*92*).

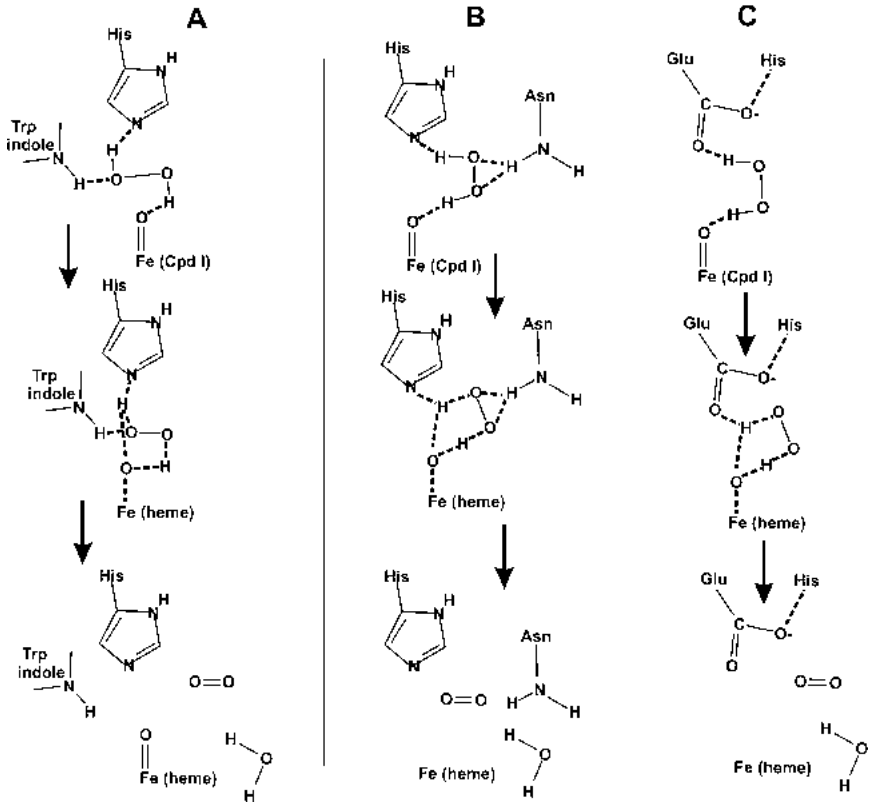

FIG. 19. Mechanisms of compound I reduction in type B catalases (based on yeast CCP) (see also Section IV,F and Fig. 7) (**A**); type A catalases (**B**); and chloroperoxidase (**C**).

The reduction of compound I in chloroperoxidase differs from both of the mechanisms in type A and B catalases because of there being only a single glutamic acid residue to catalyze the reaction. The reducing hydrogen peroxide must initially bind with the glutamate side chain and the oxyferryl oxygen. The highly electronegative glutamate will easily extract a proton from the peroxide, but it is more difficult to conceive of a hydrogen or reducing equivalent being transferred to it. Two options might be considered. In the first, the hydrogen peroxide is highly polarized by the glutamate, resulting in a hydride transfer to the oxyferryl oxygen and simultaneous proton transfer to the glutamate. The proton on the glutamate would ultimately be transferred to the Fe^{II}—O—H^- to produce water and native enzyme. In the second option, a single reducing equivalent, a hydrogen, is transferred to the oxyferryl oxygen. The second reducing equivalent and proton are transferred to the glutamate and delocalized in the intricate complex involving Glu183, His105, the propionate chains, and the Mn^{II} cation. This equivalent is then transferred back to the Fe^{IV}—O—H to complete the reaction (Fig. 19C). Obviously, the presence of glutamate alone on the distal side does not present the optimal catalytic site for reaction with hydrogen peroxide, explaining the low reactivity.

IX. Summary

Catalases continue to present a challenge and are an object of interest to the biochemist despite more than 100 years of study. More than 120 sequences, seven crystal structures, and a wealth of kinetic and physiological data are currently available, from which considerable insight into the catalytic mechanism has been gained. Indeed, even the crystal structures of some of the presumed reaction intermediates are available. This body of information continues to accumulate almost daily.

Have we exhausted catalases as a source of information about protein structure and the catalatic mechanisms? The answer is clearly no. With each structure reported comes new information, often including structural modifications seemingly unique to catalases and with roles that remain to be explained. Despite a deeply buried active site, catalases exhibit one of the fastest turnover rates determined. This presents the as yet unanswered question of how substrate can access the active site while products are simultaneously exhausted with a potential turnover rate of up to 10^6 per second. The complex folding pathway that produces the intricate interwoven arrangement of subunits also remains to be fully clarified.

The catalase-peroxidases present other challenges. More than 20 sequences are available, and interest in the enzyme arising from its involvement in the process of antibiotic sensitivity in tuberculosis-causing bacteria has resulted in a considerable body of kinetic and physiological information. Unfortunately, the determination of crystallization conditions and crystals remain an elusive goal, precluding the determination of a crystal structure. Furthermore, the presence of two possible reaction pathways, peroxidatic and catalatic, has complicated a definition of the reaction mechanisms and the identity of catalytic intermediates. There is work here to occupy biochemists for many more years.

ACKNOWLEDGMENTS

This work was supported by operating grants from the Natural Sciences and Engineering Research Council of Canada (NSERC) to PCL and PN. The assistance of J. Switala, B. Tattrie, and M. Maj over the years is appreciated. Receipt of preprints in advance of their publication from C. Obinger is also appreciated.

REFERENCES

1. Loew, O. *U.S. Dept of Agri. Repts*. **1900,** *65,* 5.
2. Loewen, P. C. In "Oxidative Stress and the Molecular Biology of Antioxidant Defenses"; Scandalios, J. G., ed.; pp. 273–308. Cold Spring Harbor Laboratory Press: Cold Spring Harbor, NY, 1997.
3. Zamocky, M.; Koller, F. *Prog. Biophys. Molec. Biol*. **1999,** *72,* 19.
4. Kremer, M. L. *Trans. Faraday Soc*. **1965,** *61,* 1453.
5. Keilin, D.; Hartree, E. F. *Nature* **1950,** *160,* 513.
6. Klotz, M. G.; Klassen, G. R.; Loewen, P. C. *Mol. Biol Evol*. **1997,** *14,* 951.
7. Welinder, K. *Curr. Opin. Struc. Biol*. **1992,** *2,* 388.
8. Kono, Y.; Fridovich, I. *J. Biol. Chem*. **1983,** *258,* 6015.
9. Allgood, G. S.; Perry, J. J. *J. Bacteriol*. **1986,** *168,* 563.
10. Waldo, G. S.; Fronko, R. M.; Penner-Hahn, J. E. *Biochemistry* **1991,** *30,* 10486.
11. Whittaker, M. M.; Barynin, V. V.; Antonyuk, S. V.; Whittaker, J. W. *Biochemistry* **1999,** *38,* 9126.
12. Arnao, M. B.; Acosta, M.; del Rio, J. A.; Varn, R.; Garcia-Canovas, F. *Biochim. Biophys. Acta* **1990,** *1041,* 43.
13. Thomas, J. A.; Morris, D. R.; Hager, L. P. *J. Biol. Chem*. **1970,** *245,* 3129.
14. Sundaramoorthy, M.; Terner, J.; Poulos, T. L. *Structure* **1995,** *3,* 1367.
15. Sun, W.; Kadima, T. A.; Pickard, M. A.; Dunford, H. B. *Biochem. Cell. Biol*. **1994,** *72,* 321.
16. Facey, S.; Gross, F.; Vining, L. C.; Yang, K.; van Pee, K. H. *Microbiology* **1996,** *142,* 657.
17. Mulvey, M. R.; Switala, J.; Borys, A.; Loewen, P. C. *J. Bacteriol*. **1990,** *172,* 6713.
18. Ma, M.; Eaton, J. W. *Proc. Nat. Acad. Sci. USA* **1992,** *89,* 7924.

19. Nicholls, P. *Biochim. Biophys. Acta*. **1965,** *99,* 286.
20. Nicholls, P. *Biochim. Biophys. Acta* **1972,** *279,* 306.
21. Clayton, R. K. *Biochim. Biophys. Acta*. **1960,** *36,* 35.
22. Nicholls, P.; Schonbaum, G. R. In "The Enzymes"; P. Boyer; H. Lardy; K. Myrback, eds.; Vol. VIII, 2nd ed., pp. 147–225; Academic Press: New York, 1963.
23. Aebi, H.; Heiniger, J.-P.; Suter, H. *Experientia* **1962,** *18,* 129.
24. Aebi, H.; Cantz, M.; Suter, H. *Experientia* **1965,** *21,* 713.
25. Deisseroth, A.; Dounce, A. L. *Physiol. Rev*. **1970,** *50,* 319.
26. Ruis, H.; Koller, F. In "Oxidative Stress and the Molecular Biology of Antioxidant Defenses"; Scandalios, J. G., ed.; pp. 309–342. Cold Spring Harbor Laboratory Press: Cold Spring Harbor, NY, 1997.
27. Scandalios, J. G., Guan, L.; Polidoros, A. N. In "Oxidative Stress and the Molecular Biology of Antioxidant Defenses"; Scandalios, J. G., ed.; pp. 343–406. Cold Spring Harbor Laboratory Press: Cold Spring Harbor, NY, 1997.
28. Loewen, P. C.; Switala, J.; Triggs-Raine, B. L. *Arch. Biochem. Biophys*. **1985,** *243,* 144.
29. Christman, M. F.; Storz, G.; Ames, B. N. *Proc. Natl. Acad. Sci. USA* **1989,** *86,* 3484.
30. Ivanova, A.; Miller, C.; Glinsky, G.; Eisenstark, A. *Molec. Microbiol*. **1994,** *12,* 571.
31. Mukhopadhyay, S.; Schellhorn, H. E. *J. Bacteriol*. **1994,** *176,* 2300.
32. Visick, J. E.; Clark, S. *J. Bacteriol*. **1997,** *179,* 3158.
33. Loewen, P. C.; Hennge-Aronis, R. *Ann. Rev. Microbiol*. **1994,** *48,* 53.
34. Bonnichsen, R. K.; Chance, B.; Theorell, H. *Acta Chem. Scand*. **1947,** *1,* 685.
35. Beers, R. F.; Sizer, I. W. *J. Biol. Chem*. **1952,** *195,* 133.
36. Ogura, Y. *Arch. Biochem. Biophys*. **1955,** *57,* 288.
37. Keilin, D.; Nicholls, P. *Biochim. Biophys. Acta* **1958,** *29,* 302.
38. Fita, I.; Rossmann, M. G. *J. Mol. Biol*. **1985,** *185,* 21.
39. Brill, A. S.; Castleman, B. W.; McKnight, M. E. *Biochemistry* **1976,** *15,* 2209.
40. Nicholls, P. *Biochem. J*. **1961,** *81,* 365.
41. Maj, M.; Loewen, P. C.; Nicholls, P. *Biochim. Biophys. Acta* **1998,** *1384,* 209.
42. Young, L. J.; Siegel, L. M. *Biochemistry* **1988,** *27,* 2790.
43. Nicholls, P. *Biochem. J.* **1964,** *90,* 331.
44. Nicholls, P. *Trans. Farad. Soc.* **1964,** *60,* 137.
45. Kalynaraman, B.; Janzen, E. G.; Mason, R. P. *J. Biol. Chem*. **1985,** *260,* 4003.
46. Lardinois, O.; Rouxhet, P. G. *Biochim. Biophys. Acta* **1996,** *1298,* 180.
47. Hillar, A.; Nicholls, P. *FEBS Lett*. **1992,** *314,* 179.
48. Kirkman, H. N.; Gaetani, G. F. *Proc. Natl. Acad. Sci. USA* **1984,** *81,* 4343.
49. Nicholls, P. *Biochim. Biophys. Acta*. **1964,** *81,* 479.
50. Fita, I.; Rossmann, M.G. *Proc. Natl. Acad. Sci. USA* **1985,** *82,* 1604.
51. Bicout, D. J.; Field, M. J.; Gouet, P.; Jouve, H.-M. *Biochim. Biophys. Acta* **1995,** *1252,* 172.
52. Olson, L. P.; Bruice, T. C. *Biochemistry* **1995,** *34,* 7335.
53. Almarsson, O.; Sinha, A.; Gopinath, E.; Bruice, T. C. *J. Amer. Chem. Soc*. **1993,** *115,* 7093.
54. Kirkman, H. N.; Rolfo, M.; Ferraris, A. M.; Gaetani, G. F. *J. Biol. Chem*. **1999,** *274,* 13908.
55. Hayashi, Y.; Yamazaki, I. *J. Biol Chem*. **1979,** *254,* 9101.
56. He, B.; Sinclair, R.; Copeland, B. R.; Makino, R.; Powers, L. S.; Yamazaki, I. *Biochemistry* **1996,** *35,* 2413.
57. DeFelippis, M. R.; Murthy, C. P.; Faraggi, M.; Klapper, M. H. *Biochemistry* **1989,** *28,* 4847.

58. Hillar, A.; Nicholls, P.; Switala, J. Loewen, P. C. *Biochem. J*. **1994,** *300,* 531.
59. Jouve, H. M.; Pelmont, J.; Gaillard, J. *Arch. Biochem. Biophys*. **1986,** *248,* 71.
60. Claiborne, A.; Malinowski, D. P.; Fridovich, I. *J. Biol. Chem*. **1979,** *254,* 11664.
61. Hochman, A.; Shemesh, A. *J. Biol. Chem*. **1987,** *262,* 6871.
62. Loewen, P. C.; Stauffer, G. V. *Mol. Gen. Genet*. **1990,** *224,* 147.
63. Welinder, K. *Biochim. Biophys. Acta* **1991,** *1080,* 215.
64. Percy, M. E. *Can. J. Biochem. Cell. Biol*. **1984,** *62,* 1006.
65. Hochman, A.; Shemesh, A. *J. Biol. Chem*. **1987,** *262,* 6871.
66. Goldberg, I.; Hochman, A. *Biochim. Biophys. Acta* **1989,** *991,* 330.
67. Hochman, A.; Goldberg, I. *Biochim. Biophys. Acta* **1991,** *1077,* 299.
68. Goldberg, I.; Hochman, A. *Arch. Biochim. Biophys*. **1989,** *268,* 124.
69. Levy, E.; Eyal, Z.; Hochman, A. *Arch. Biochim. Biophys*. **1992,** *296,* 321.
70. Obinger, C.; Regelsberger, G.; Strasser, G.; Burner, U.; Peschek, G. A. *Biochem. Biophys. Res. Commun*. **1997,** *235,* 545.
71. Regelsberger, G.; Jakopitsch, C.; Engleder, M.; Rüker, F.; Peschek, G. A.; Obinger, C. *Biochemistry* **1999,** *38,* 10480.
72. Jakopitsch, C.; Rüker, F.; Regelsberger, G.; Tockal, M.; Peschek, G.; Obinger, C. *Biol. Chem*. **1999,** *380,* in press.
73. Murthy, M. R. N.; Reid, T. J.; Sicignano, A.; Tanaka, N.; Rossmann, M. G. *J. Mol. Biol.* **1981,** *152,* 465.
74. Fita, I.; Silva, A. M.; Murthy, M. R. N.; Rossmann, M. G. *Acta Cryst. B* **1986,** *42,* 497.
75. Berthet, S.; Nykyri, L. M.; Bravo, J.; Berthet-Colominas, C.; Alzari, P.; Koller, F.; Fita, I. *Protein Sci*. **1997,** *6,* 481.
76. Mate, M. J.; Zamocky, M.; Nykyri, L. M.; Herzog, C.; Alzari, P. M.; Betzel, C.; Koller, F.; Fita, I. *J. Mol. Biol*. **1999,** *286,* 135.
77. Gouet, P.; Jouve, H. M.; Dideberg, O. *J. Mol. Biol*. **1995,** *249,* 933.
78. Murshudov, G. N.; Melik-Adamyan, W. R.; Grebenko, A. I.; Barynin, V. V.; Vagin, A. A.; Vainshtein, B.K.; Dauter, Z.; Wilson, K. *FEBS Lett*. **1992,** *312,* 127.
79. Vainshtein, B. K.; Melik-Adamyan, W. R.; Barynin, V. V.; Vagin, A. A.; Grebenko, A. I. *Nature* **1981,** *293,* 1981, 411.
80. Vainshtein, B. K.; Melik-Adamyan, W. R.; Barynin, V. V.; Vagin, A. A.; Grebenko, A. I.; Borisov, V. V.; Bartels, K. S.; Fita, I.; Rossmann, M. G. *J. Mol. Biol*. **1986,** *188,* 49.
81. Bravo, J.; Verdaguer, N.; Tormo, J.; Betzel, C.; Switala, J.; Loewen, P. C.; Fita, I. *Structure* **1995,** *3,* 491.
82. Bravo, J.; Mate, M. J.; Schneider, T.; Switala, J.; Wilson, K.; Loewen, P. C.; Fita, I. *Proteins* **1999,** *34,* 155.
83. Bravo, J.; Fita, I.; Gouet, P.; Jouve, H. M.; Melik-Adamyan, W.; Murshudov, G. N. In "Oxidative Stress and the Molecular Biology of Antioxidant Defenses"; Scandalios, J. G., ed.; pp. 407–445. Cold Spring Harbor Laboratory Press, Cold Spring Harbor, NY, 1997.
84. Sevinc, M. S.; Switala, J.; Bravo, J.; Fita, I.; Loewen, P. C. *Prot. Eng*. **1998,** *11,* 549.
85. Loewen, P. C.; Switala, J. Biochem. *Cell Biol*. **1986,** *64,* 638.
86. Switala, J.; O´Neil, J.; Loewen, P. C. *Biochemistry* **1999,** *38,* 3895.
87. Bergdoll, M.; Remy, M. H.; Cagon, C.; Masson, J. M.; Dumas, P. *Structure,* **1997,** *4,* 391.
88. Tanford, C.; Lovrien, R. *J. Am. Chem. Soc*. **1962,** *84,* 1892.
89. Ruis, H. Can. *J. Biochem*. **1979,** *57,* 1122.
90. Hook, D. W. A.; Harding, J. J. *Eur. J. Biochem*. **1997,** *247,* 380.
91. Murshudov, G. N.; Grebenko, A. I.; Barynin, V.; Dauter, Z.; Wilson, K.; Vainshtein,

B. K.; Melik-Adamyan, W.; Bravo, J.; Ferran, J. M.; Switala, J.; Loewen, P. C.; Fita, I. *J. Biol. Chem*. **1996,** *271,* 8863.
92. Loewen, P. C.; Switala, J.; von Ossowski, I.; Hillar, A.; Christie, A.; Tattrie, B.; Nicholls, P. *Biochemistry* **1993,** *32,* 10159.
93. Bravo, J.; Fita, I.; Ferrer, J. C.; Ens, W.; Hillar, A.; Switala, J.; Loewen, P. C. *Protein Sci*., **1997,** *6,* 1016.
94. Mate, M. J.; Sevinc, M. S.; Hu, B.; Bujons, J.; Bravo, J.; Switala, J.; Ens, W.; Loewen, P. C.; Fita, I. *J. Biol. Chem*. **1999,** *274,* 27717.
95. Sevinc, M. S.; Mate, M. J.; Switala, J.; Fita, I.; Loewen; P. C. *Protein Sci*. **1999,** *8,* 490.
96. Zamocky, M.; Herzog, C.; Nykyri, L. M.; Koller, F. *FEBS Lett*. **1995,** *367,* 241.
97. Gouet, P.; Jouve, H. M.; Williams, P. A.; Andreoletti, P.; Nussaume, L.; Hadju, J. *Nature Struct. Biol*. **1996,** *3,* 951.
98. Bell, C. E.; Yeates, T. O.; Eisenberg, D. *Protein Sci*. **1997,** *6,* 2084.
99. Tanner, J. J.; Tu, S. C.; Barbour, L. J.; Barnes, C. L.; Krause, K. L. *Protein Sci*. **1999,** *8,* 1725.
100. Sevinc, S.; Ens, W.; Loewen, P. C. *Eur. J. Biochem* **1995,** *230,* 127.
101. Hillar, A. Ph.D. Thesis, 1999, University of Manitoba, Winnipeg, MB, Canada.
102. Poulos, T. L.; Kraut, J. *J. Biol. Chem*. **1980,** *255,* 8199.
103. English, A. M.; Tsaprailis, G. *Adv. Inorg. Chem*. **1996,** *43,* 79.
104. Dunford, H. B. In "Heme Peroxidases." J. Wiley & Sons: New York, 1999.